MARMARA UNIVERSITY
INSTITUTE FOR GRADUATE STUDIES IN PURE AND APPLIED SCIENCES

TYROSINASE-BASED MELANIN PRODUCTION IN *CORYNEBACTERIUM GLUTAMICUM*

CEREN KARCIOĞLU

MASTER THESIS
Department of Bioengineering

Thesis Supervisor
Prof. Dr. Berna Sarıyar AKBULUT

Thesis CO- Supervisor
Prof. Dr. Dilek KAZAN

ISTANBUL, 2024

MARMARA UNIVERSITY
INSTITUTE FOR GRADUATE STUDIES IN PURE AND APPLIED SCIENCES

TYROSINASE-BASED MELANIN PRODUCTION IN *CORYNEBACTERIUM GLUTAMICUM*

CEREN KARCIOĞLU

524221010

MASTER THESIS
Department of Bioengineering

Thesis Supervisor
Prof. Dr. Berna Sarıyar AKBULUT

Thesis CO- Supervisor
Prof. Dr. Dilek KAZAN

ISTANBUL, 2024

ACKNOWLEDGEMENT

I would like to express my deepest gratitude towards my supervisors Prof. Dr. Berna Sarıyar Akbulut and Assoc. Prof. Dr. Dilek Kazan, for their immense support and encouragement. They have always been kind, understanding, and positive throughout my research. It was an honour to be their student and learn from them. This study was supported by the Scientific and Technological Research Council of Turkey (TUBITAK) under the Grant Number 120N728 and the Marmara University Scientific Research Projects Committee (BAPKO) under the Grant Number FYL-2023-10911. CK was supported by the TUBITAK-BIDEB 2210-D fellowship.

I am so thankful for especially my entire family Sibel, Taner, and Eren Karcioglu, and my endless love Taha Ulukaya for their endless love, support, and motivation. They have always believed in me, which kept me going through the path of my master's degree. Also, my endless love encouraged me and gave me emotional support during my studies. This accomplishment wouldn't be possible without the support of all my family.

I am so grateful to thank the entire laboratory group of Prof. Dr. Berna Sarıyar Akbulut. They have always been there throughout my Master's journey and have given me strength and support at every step of the way.

March 2024 **Ceren KARCIOGLU**

TABLE OF CONTENTS

ACKNOWLEDGEMENT ..... **i**
TABLE OF CONTENTS ..... **ii**
ÖZET ..... **v**
ABSTRACT ..... **vi**
LIST OF ..... **vii**
1. SYMBOLS ..... **vii**
ABBREVIATIONS ..... **viii**
LIST OF FIGURES ..... **ix**
LIST OF TABLES ..... **x**
1. INTRODUCTION **1**
1.1. Melanin 1
1.2. Melanin Production 3
1.3. Chemical Synthesis 6
1.4. Extraction From Conventional Natural Sources 6
1.5. Microbial Production 7
1.6. Limitations of Microbial Melanin In Commercialization and Industrial Uses 9
1.7. Applications of Melanin 10
1.8. Melanin Analysis 11
1.9. Metabolic Engineering 12
1.10. *Corynebacterium Glutamicum* 13
1.11. Renewable Carbon Source 14
1.11.1. Orange peel hydrolysate 14
1.12. Model Based Optimization 15
2. MATERIALS AND METHODS **16**
2.1. Materials 16
2.1.1. Strains 16
2.1.2. Chemicals 16
2.1.3. Buffers and media 17
2.2. Methods 18
2.2.1. Experimental techniques 18
2.2.1.1. Cultivation conditions 18

2.2.1.2. Fermentative melanin production with Cg-EKV-I 19
2.2.1.3. Fermentative melanin production with AROM3D 20
2.2.1.4. Melanin production from orange peels sugar extract in Cg-EKV-II.....20
2.3. Melanin Extraction 21
2.4. Melanin Quantification 21
2.5. Analysis of melanin with High Performance Liquid Chromatography.....21
2.6. Analysis of L-tyr High Performance Liquid Chromatography.....21
2.7. Analysis of melanin with UV-Vis Spectrophotometry.....22
2.8. Analysis of melanin with Fourier Transform Infrared Microscopy (FT/IR) 22
2.9. Analysis of melanin with scanning electron microscopy (SEM) 22
2.10. Whole cell biocatalysts with orange peel hydrolysate.....23
2.11. Model based optimization.....23
2.11.1. Design of experiments 23
2.11.2. Modelling and optimization 23
3. RESULTS AND DISCUSSION 25
3.1. Melanin production with Cg-EKV-I.....25
3.1.1. Effect of different copper ion concentrations.....25
3.1.2. Effect of different flask volumes.....26
3.1.3. Effect of different rotation speeds 26
3.1.4. Effect of different additional L-Tyr.....27
3.1.5. Effect of flask geometry.....28
3.1.6. Summary with CgEKV-I cells 29
3.2. Melanin production with AROM3D.....29
3.2.1. Effect of copper addition time and L-Phe concentration 30
3.2.2. Effect of copper and L-Phe concentration on melanin production.....31
3.2.3. Growth curve analysis with dissolved oxygen measurement 32
3.3. The model-based optimization for Kriging and Quadratic model 33
3.3.1. Experimental results of central composite design 33
3.3.2. Experimental results of random sampling 35
3.3.3. Model based optimization for melanin production.....37
3.4. Purification of melanin 39
3.5. Melanin analysis.....40
3.5.1. HPLC analysis of melanin 40

3.5.2. UV-Vis analysis of melanin 40
3.5.3. FT/IR analysis of melanin 41
3.5.4. SEM analysis of melanin 42
3.6. Melanin production with orange peel hydrolysate with Cg-EKV-II 43
4. CONCLUSION 45
REFERENCES 47
APPENDIX A – Raw data on Cg-EKV-I 60
APPENDIX B – Kriging and Quadratic model selected data 64
APPENDIX C – OD_{600} results 66
APPENDIX D – HPLC results 68
CURRICULUM VITAE /ÖZGEÇMİŞ 69

ÖZET

CORYNEBACTERIUM GLUTAMICUM İLE TİROZİNAZA BAĞLI MELANİN ÜRETİMİ

Tahmini olarak 30 milyar doları aşan değeri ile pigmentler, dünya çapında büyük bir ekonomik öneme sahiptir. Bu pigmentlerden biri olan melanin, kimyasal yapısına göre 4 farklı kategoriye ayrılır: eumelanin, feomelanin, nöromelanin ve allomelanin. Eumelanin, siyah ila kahverengi tonlarda ve tirozinin L-3,4-dihidroksifenilalanine (L-DOPA) oksidatif polimerizasyon türevleri ile oluşturulan melanin bir alt grubu olarak kabul edilir. Eumelanin üreten kaynaklardan biri, öncüleri tirozin veya L-DOPA olan bakterilerdir. Bu tezde ekonomik melanin pigmentinin üretimi için üç farklı *Corynebacterium glutamicum* hücresinde üretim araştırılmıştır. İlk olarak, Cg-EKV-I hücresi kullanılarak tirozinaz tarafından besi yerine ilave edilen tirozin L-DOPA'ya dönüştürülmüş ve sonrasında L-DOPA dopakinon'a dönüşmüştür. Dopakinon kendiliğinden okside olmuş ve melanin polimerleri oluşmuştur. Önce bu hücre ile melaninin optimum eldesi, üretim şişesi şekli, üretim hacmi ve rotasyon hızı incelenerek belirlenmiştir. Ek olarak, üretime başladıktan 24 saat sonra, toz L-tirozin eklenerek ilave edilen tirozinin üretime ne kadar katkı sağladığı incelenmiştir. Elde edilen deneysel sonuçlar tirozin üreticisi AROM3D hücresiyle üretim için kullanılmıştır. Modelleme temelli optimizasyon ile AROM3D hücrelerinin maksimum melanin üretim koşulları belirlenmiştir. Tirozin ilavesi ile Cg-EKV-I hücreleri elde edilen maksimum melanin üretimi 0.75 g/L iken, tirozin ilavesi olmadan AROM3D hücresinden optimizasyon sonrasında elde edilen melanin üretimi 1.03 g/L olmuştur. Optimizasyon sonrasında elde edilen melanin saflaştırılmıştır. Üretilen bu pigmentin melanin olduğu HPLC, UV-Vis, FT/IR ve SEM analizleri ile gösterilmiştir. Son olarak, Cg-EKV-II hücresi ile portakal kabuğu hidrolizi kullanılarak melanin üretimi gerçekleştirilmiştir. Hücre miktarı, sıcaklık ve rotasyon hızı optimize edilmiştir. Bu tez çalışmasıyla, melanin pigmentinin optimum ve ekonomik olarak uygun bir şekilde elde edilmesi sağlanmıştır.

ABSTRACT

TYROSINASE-BASED MELANIN PRODUCTION IN *CORYNEBACTERIUM GLUTAMICUM*

Pigments, with an estimated value surpassing 30 billion dollars in the industry, hold significant economic importance worldwide. Melanin, one of these pigments, is categorized into four distinct types based on its chemical structure: eumelanin, pheomelanin, neuromelanin, and allomelanin. Eumelanin, ranging from black to brown tones, is considered a subcategory of melanin formed by oxidative polymerization derivatives of tyrosine such as L-3,4-dihydroxyphenylalanine (L-DOPA). One of the sources producing eumelanin is bacteria with precursors like tyrosine or L-DOPA. This thesis investigates the production of economical melanin pigment using three different Corynebacterium glutamicum cells. Initially, using the Cg-EKV-I cell, tyrosine added instead of a growth medium is converted to L-DOPA by tyrosinase and subsequently L-DOPA transforms into dopaquinone. Dopaquinone undergoes auto-oxidation, resulting in the formation of melanin polymers. The optimal conditions for melanin production with this cell, including production vessel shape, volume, and rotation speed, were determined. Additionally, the contribution of added tyrosine to production was examined by adding powdered L-tyrosine 24 hours after the start of production. The experimental results were used for production with the tyrosine-producing AROM3D cell. Using modeling-based optimization, the maximum melanin production conditions for AROM3D cells were determined. While the maximum melanin production from Cg-EKV-I cells with tyrosine addition was 0.75 g/L, the melanin production after optimization from AROM3D cells without tyrosine addition was 1.03 g/L. The obtained melanin was purified after optimization. The produced pigment's identification as melanin was confirmed through HPLC, UV-Vis, FT/IR, and SEM analyses. Lastly, melanin production was attempted using orange peel hydrolysate with the Cg-EKV-II cell, with optimization of cell amount, temperature, and rotation speed. This thesis ensures the optimum and economically feasible production of melanin pigment.

LIST OF SYMBOLS

%	**:**	Percentage
°C	**:**	Celcius
cm	**:**	Centimeter
g	**:**	Gram
h	**:**	Hour
L	**:**	Liter
M	**:**	Molar
mg	**:**	Milligram
min	**:**	Minute
mL	**:**	Milliliter
mM	**:**	Millimolar
rpm	**:**	Revolution per minute
w	**:**	Weight
µg	**:**	Microgram
µl	**:**	Microliter
mg/L	**:**	Miligram per liter
g/L	**:**	Gram per liter
mg/mg	**:**	Miligram per miligram

ABBREVIATIONS

BHI	**:**	Brain Heart Infusion
Cg	**:**	*C. glutamicum* ATCC 13032
Cg-EKV-I	**:**	C. glutamicum ATCC 13032 harbouring pEKEx2-tyrRs
Cg-EKV-II	**:**	EKV-I harbouring pEKEx3-xylAXc-xylBCg
AROM3D	**:**	AROM3 harbouring pEKEx3-tyrRs
Km	**:**	Kanamycin
MOPS	**:**	3-morpholinopropanesulfonic acid
PKS	**:**	Protocatechuic Acid
Spec	**:**	Spectinomycin
RSM	**:**	Response Surface Methodology
L-DOPA	**:**	L-3,4-dihidroksifenilalanin
L-Tyr	**:**	L-tyrosine
DHN	**:**	1,8-dihydroxynaphthalene
FT/IR	**:**	Fourier Transform Infrared Microscopy
SEM	**:**	Scanning electron microscopy
HPLC	**:**	High performance liquid chromatography
L-Phe	**:**	L-phenylalanine
Cu	**:**	Copper sulfate pentahydrate
Uv/Vis analysis	**:**	Ultraviolet visible analysis
IPTG	**:**	Isopropyl β-Dithiogalactopyranoside

LIST OF FIGURES

Figure 1.1 Synthetic melanin types adapted from 2
Figure 1.2 Chemical structure of melanin from *Sepia officinalis* 3
Figure 1.3 Mild and harsh procedures employed for extracting melanin from living cells. 7
Figure 1.4 The schematic representation that illustrates melanin synthesis, highlighting important chemical transformations shared among microbial melanin-building processes in bacteria and fungi. The pathways depicted include the DHN-pathway (a) and the DOPA-pathway (b). In cases of enzymatic imbalances (c), altered metabolic pathways may result in the formation of different types of melanins, such as pyomelanin 8
Figure 1.5 Applications of microbial melanin 10
Figure 3.1 AROM3D oxygen measurement in PreSense. Both productions set up with 0.1 mM copper ions and 0.5 mM L-Phe concentration. The dots: Copper ions added initially, the triangle: Copper ions added after 24 hours.....33
Figure 3.2 A) 1 g/L Standard melanin analysis B) 1 g/L purified melanin with HPLC at 50 °C.....40
Figure 3.3 Relationship between log absorbance and wavelength from 200 to 800 nm on purified melanin. The lines show 0.25 g/L, the triangles show 0.125 g/L, the squares show 0.1 g/L, and the dots show 0.05 g/L of purified melanin. 41
Figure 3.4 A) FTIR analysis of melanin (Kiran., 2017) B) Analysis of purified melanin .42
Figure 3.5 Images obtained from SEM with purified melanin. (Magnitude 15000x, size 5µm) 43

LIST OF TABLES

Table 1.1 The summary of general melanins, sources, and their related precursor 1
Table 1.2 General melanin production 4
Table 2.1 List of strains and descriptions 16
Table 2.2 List of media and buffers used. 18
Table 3.1 Effect of different copper ion concentrations for Cg-EKV-I 25
Table 3.2 Effect of culture volume on melanin production with Cg-EKV-I.....26
Table 3.3 Effect of rotation speed on melanin production by Cg-EKV-I with 0.1 mM copper ions 27
Table 3.4 0.2 mM copper concentration at 120, 150, and 200 rpm with Cg-EKV-I on melanin production 27
Table 3.5 Effect of additional 4 g/L L-Tyr supplement at different times for melanin production by CgEKV-I (yield on L-Tyr). 28
Table 3.6 Effect of different flask geometries for Cg-EKV-I 29
Table 3.7 Melanin production with 0.25 or 0.5 L-Phe and 0.1 mM copper at t_0 and t_{24} ..30
Table 3.8 0.1 mM copper ion and 0.125, 0.25, 0.50 mM L-Phe concentrations were added initially with AROM3D on melanin production. 31
Table 3.9 0.2 mM copper ions and 0.125, 0.25, 0.50 mM L-Phe concentrations were added initially with AROM3D on melanin production. 32
Table 3.10 0.3 mM copper ions and 0.125, 0.25, 0.50 mM L-Phe concentrations were added initially with AROM3D on melanin production. 32
Table 3.11 Titers obtained from points selected by central composite design. 34
Table 3.12 Titers obtained from randomly selected points. 35
Table 3.13 Actual melanin titers under optimal conditions (initially added copper ion and 0.5 mM L-Phe). 38
Table 3.14 The yields result from the purification of melanin with different growth conditions. 39
Table 3.15 Whole-cell bio-fermentation melanin production with CgEKV-II after 24 hours with 100 µL copper ions. 43

1. INTRODUCTION

1.1. Melanin

Melanin is a heterogeneous pigment produced by organisms from bacteria to mammals. In humans, melanin is significantly accountable for the color of the skin and eyes (d'Ischia et al., 2015; Solano, 2014). This is generally a black or brown pigment, deriving its name from melanos, an ancient Greek term for black color (Borovanskỳ & Riley, 2011). It may also appear pink or red, such as pheomelanin found in freckles, feathers, and red hair. Melanin pigments are classified according to their chemical structure. These include eumelanin, pheomelanin, neuromelanin, and allomelanin. Different melanin types are outlined in Figure 1.1 (D'Ischia et al., 2013). The widespread origins of melanin contribute to its heterogeneity in size, color, function, and composition. Its hydrophobic nature, high molecular weight, and a highly negative charge make melanin challenging to employ classical analytical approaches for defining and characterizing its structure (I.-E. Pralea et al., 2019). In addition to exhibiting insolubility in the majority of solvents it displays resistance to chemical degradation (Nosanchuk & Casadevall, 2003; I. E. Pralea et al., 2019).

Eumelanin, the predominant melanin type in animals and humans, belongs to the black to brown subgroup of melanin pigments. It is produced through the oxidative polymerization of derivatives of the tyrosine amino acid, specifically L-3,4-dihydroxyphenylalanine (L-Dopa) (Solano., 2014). Eumelanin is crucial from both technological and biological perspectives and is extensively worked on and utilized as an example for synthetic melanin. Pheomelanin which is distinct from eumelanin due to the presence of sulphur in its composition, is commonly found in hair, freckles, and feathers. Its precursor is 5-cysteinyl-Dopa. Another melanin type is neuromelanin, which is generated inwardly human neurons through the oxidation of dopamine precursors and, also catecholamine precursors. Allomelanin is often found in fungi. This group contains various non-nitrogenous subgroups of melanin produced from different catechol and dihydroxynaphthalene precursors. Catechol melanin is produced by plants, and DHN-melanin pheomelanin is melanin produced by bacteria and fungi (Cordero & Casadevall., 2017; Eisenman & Casadevall., 2012;Tran-Ly et al., 2020). The different types of melanin are summarized in Table 1.1.

Table 1.1 The summary of general melanins, sources, and their related precursor (Tran-Ly et al., 2020).

Group of Melanin	Producing source	Melanin precursors
Eumelanin (DOPA-melanin)	Animals, bacteria, fungi	Tyrosine or L-Dopa
Pheomelanin	Animals	5-S-cys-Dopa
Neuromelanin	Human brain	Dopamine and 5-S-cys Dopamine
Catechol-melanin	Plant	Catechol
DHN-melanin	Fungi, bacteria	1,8-dihydroxynaphthalene (DHN)
Pyomelanin	Fungi, bacteria	Homogentisic acid

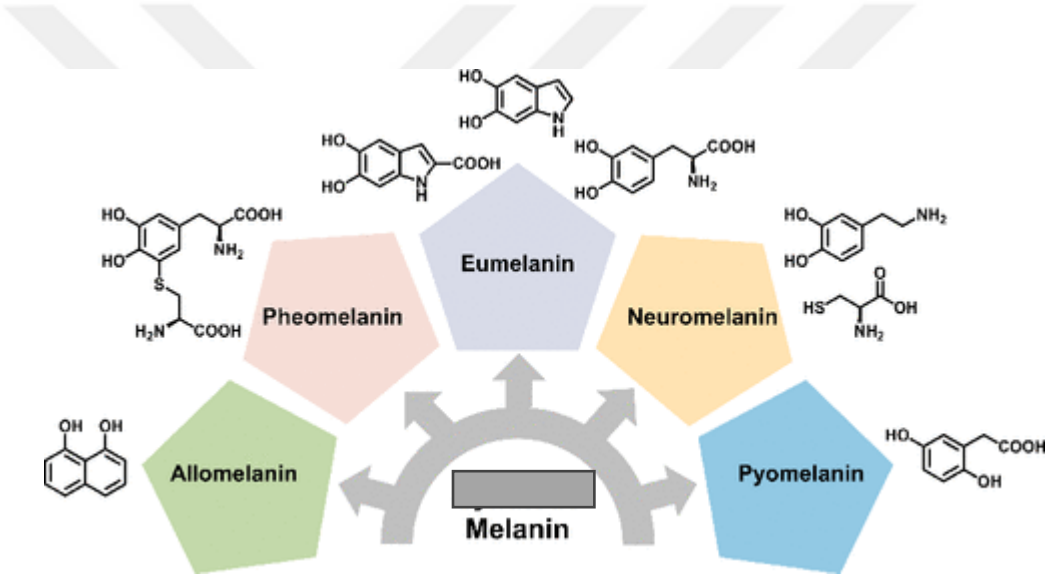

Figure 1.1 Synthetic melanin types adapted from (Cao et al., 2021)

1.2. Melanin Production

Several fruits and vegetables serve as sources of melanin, including potatoes, bananas, garlic, and apples (Hagiwara et al., 2016; Lefevre & & Perrett, 2015; Qi et al., 2020). Additionally, melanin can be extracted from plants, as demonstrated for *Mucuna monosperma* (Wight) callus (Inamdar et al., 2014). Presently, commercial melanin relies on extraction from sepia or synthetic production routes (Tran-Ly et al., 2020). The chemical structure of melanin from *Sepia officinalis* is given in Figure 1.2. Unfortunately, these methods come with several drawbacks, such as environmental pollution risks and high production costs. Alternatively, melanin production maybe achievable through microbial routes using bacteria and fungi. Thus, microbial melanin production holds significant importance due to its sustainability, relatively fast production, and scalability for mass production. Because the studies conducted by Ghadge (2020), Kazi (2022), Rudrappa (2022), Bayram (2020), Restaino (2024), El-Zawawy (2024), Polapally (2022), El-Naggar (2022), Surwase (2012), Guo J. (2014), Wang L. (2019) utilized ingredients such as starch, yeast, casein, peptone, or complex chemicals, the purification process has proven to be challenging. Additionally, in most of these studies, the supplementation of tyrosine was necessary. Furthermore, due to the utilization of mushrooms in some of these studies, as observed in the works of Saber (2023), Ribera J. (2019), Sun S. (2016), and Jalmi P. (2012), the production duration extended and became more intricate.

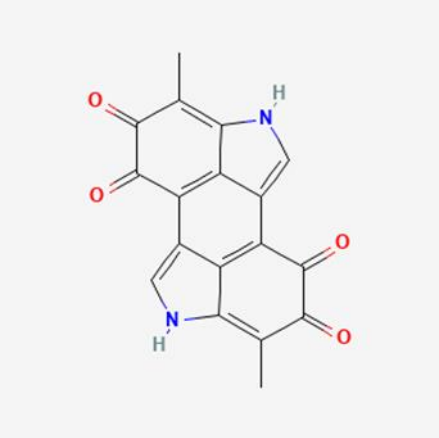

Figure 1.2 Chemical structure of melanin from *Sepia officinalis* (Melanin | C18H10N2O4 – PubChem., n.d.)

Table 1.2 General melanin production

Microorganism	Type	Melanin g / L (time /day- hour)	L-Tyr	Metal	Substrate	Reference
Bacteria						
Pseudomonas stutzeri	Dopa	6.7 (72h)	No	No	Nutrient broth, seawater	Ganesh Kumar., (2013)
Salicornia brachiata	Eumelanin	1.5 (7)	Yes	No	Starch, sodium nitrate	Ghadge., (2020)
Pseudomonas koreensis UIS 19	Eumelanin	5.5 (2)	Yes	No	Nutrient broth	Eskandari., (2021)
Streptomyces sp. BJZ10	Eumelanin	3 (2)	Yes	No	starch casein agar medium	Kazi.,(2022)
Streptomyces sp. MR28	Dopa	0.6 (10)	Yes	No	Skimmed milk powder, casein, starch	Rudrappa., (2022)
Streptomyces djakartensis NSS-3	Eumelanin	11.8 (7)	Yes	ferric ammonium citrate	Casein agar	El-Zawawy.,(2024)
Streptomyces nashvillensis DSM 40314	Dopa	0.74 (2)	No	No	Glucose, yeast	Restaino., (2024)
Streptomyces hyderabadensis 7V PT5-5R	Dopa	5.54 (7-10)	No	ferric ammonium citrate	Peptone, yeast	Ghadge., (2022)
Streptomyces parvus BSB49	Eumelanin	0.16-0.24 (4-5)	No	$CaCO_3$	Starch, yeast, dextrose	Bayram., (2020)
S. glaucescens NE AE-H	Dopa	0.35 (3-6)	No	ferric ammonium citrate	Peptone, yeast	El-Naggar., (2022)
S.roseochromogenes ATCC 13400	Eumelanin	3.94 (5)	No	No	Glucose, yeast, egagropili powder	Restaino., (2022)
S.roseochromogenes ATCC 13400	Eumelanin	9.20 (4) (batch)	No	No	Glucose, yeast, egagropili powder	Restaino., (2022)
S.puniceus RHPR9	Eumelanin	0.386 (7)	No	ferric ammonium citrate	Peptone, yeast	Polapally., (2022)
Klebsiella sp. GSK46	Eumelanin	0.13 (4)	Yes	ammoniacal silver nitrite, potassium ferricyanide	Glucose	Sajjan., (2010)
Actinoalloteichus sp. MA-32	Dopa	0.1 (7)	Yes	Fe, Mg	Glycerol	Manivasagan P., (2013)
Brevundimonas sp. SGJ	Dopa	6.8 (54h)	Yes	Cu	Tryptone	Surwase ., (2012)
Pseudomonas stutzeri HMGM-7	Dopa	7.2 (3)	Yes	No	Nutrient broth in sea water	Ganesh Kumar., (2013)
Streptomyces glaucescens NEAE-H	Dopa	0.4 (6)	yes	Fe	Protease peptone	El-Naggar NEA., (2017)
Streptomyces kathirae SC-1	Dopa	13.7 (5)	yes	Cu	Amylodextrine, yeast extract	Guo J., (2014)

Table 1.2 General melanin production (more)

Microorganism	Type	Melanin g / L (time /day- hour)	L-Tyr	Metal	Substrate	Reference
Streptomyces sp. ZL-24	Dopa	4.2 (5)	No	Fe, Ni	Soy peptone	Wang L., (2019)
S. kathirae SC-1	Dopa	13.7 (5)	Yes	NaCl, $CuSO_4$, $CaCl_2$	Amylodextrine, yeast	Guo., (2014)
Streptomyces antibioticus NRRL B-1701	Dopa	0.24 (36h)	Yes	$CuSO_4$	yeast extract, soluble starch, HAO -DBRH	Kraseasintra., (2023)
Brevundimonas sp. SGJ.	Dopa	3.81 (18h)	Yes	Cu	peptone, yeast extract, beef extract	Surwase., (2012)
S.djakartensis NSS -3	Dopa	2.83 (7)	Yes	Fe	Peptone, yeast extract, iron broth (PYI)	El-Zawawy., (2024)
Fungi						
Aureobasidium pullulans AKW	Dopa	9.295 (167.994 h)	Yes	No	Potato sucrose browth	Saber., (2023)
Aureobasidium pullulans AKW	Dopa	10.192 (167.994 h)	Yes	No	Potato sucrose broth	Saber., (2023)
Armillaria borealis	DOPA	11.58 (97)	Yes	Cu,Fe,Mg	Glucose,yeast extract	RiberaJ., (2019)
Armillaria cepistipes	DOPA	27.98 (161)	Yes	Cu,Fe,Mg	Glucose, yeast extract	Ribera J., (2019)
Armillaria ostoyae	DOPA	24.80 (153)	Yes	Cu,Fe,Mg	Glucose, yeast extract	Ribera J., (2019)
Auricularia auricula	DOPA	2.97 (8)	Yes	Cu,Fe,Mg	Lactose,yeast extract	Sun S., (2016)
Daldinia concentrica	DOPA	1.78 (73)	Yes	Cu,Fe,Mg	Glucose,yeast extract	Ribera J., (2019)
Gliocephalotrichum simplex	DOPA	6.60 (6)	Yes	Cu,Fe	Peptone,yeast extract	Jalmi P., (2012)

1.3. Chemical Synthesis

In chemical melanin synthesis, polydopamine and natural melanin exhibit similarities due to their shared functional groups, namely imine, catechol, and amine groups (Solano, 2017). These groups are synthesized through the oxidative polymerization of dopamine. Three primary approaches are employed for polydopamine synthesis: solution oxidation (1), enzymatic oxidation (2), and electro polymerization (3) (Liu et al., 2014). The solution oxidation approach, which is carried out in an alkaline environment, entails oxidation using oxygen. Alternatively, it can be synthesized by auto-polymerization of dopamine monomers. The alternative method includes the enzymatic oxidation of L-tyrosine facilitated by the tyrosinase enzyme. Besides, the diphenolic groups of dopamine may undergo oxidation, and then later polymerization onto polydopamine with the help of a laccase. The last approach is used to form polydopamine on an electrode. One drawback of this method is that polydopamine deposition is typically limited to conductive materials, as the electrode surface must be conductive (Tran-Ly et al., 2020).

1.4. Extraction From Conventional Natural Sources

Traditionally, melanin may be obtained from two sources: sepia ink or from dark hair and feathers of animals. However, these sources pose challenges for melanin extraction and production due to the tight binding of melanin to cellular components within melanosomes (Prota, 1995). Consequently, the isolation steps for melanin often involve rigorous chemical treatments to eliminate cell debris, protein fractions, and unconsumed nutrients. Usually, these procedures involve thorough hydrolysis through boiling acids or bases, followed by rinsing steps using organic solvents (I.-E. Pralea et al., 2019; Wakamatsu et al., 2003). Unfortunately, these procedures can lead to chemical changes and give damage to the melanin polymeric skeleton (I. E. Pralea et al., 2019). An alternative method reported employs gentler isolation techniques like mechanical separation using ultracentrifugation, proteolytic digestion aided by enzymes, or a combination of these methods (Novellino et al., 2000). Natural melanin has limited potential for modification, being a complete polymer. Additionally, the drying method used significantly influences the physical characteristics of melanin, such as its tendency to aggregate, surface area-to-mass ratio, and porosity (Tran-Ly et al., 2020). A summary of the two melanin extraction methods is outlined in Figure 1.3.

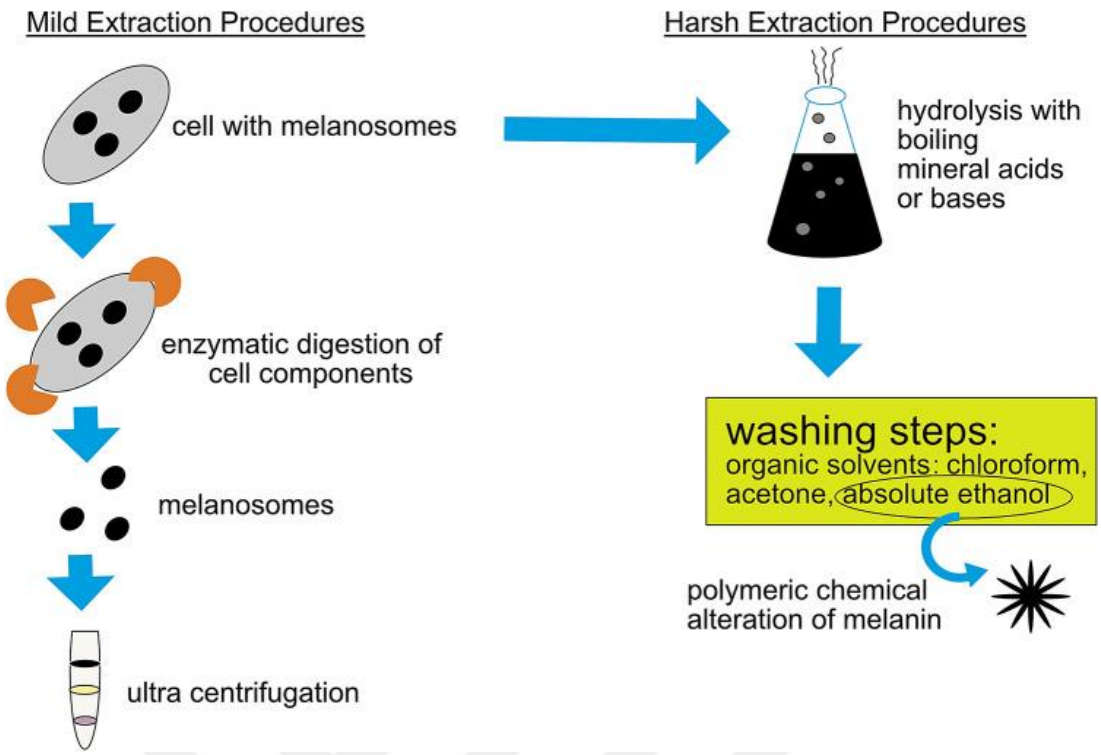

Figure 1.3 Mild and harsh procedures employed for extracting melanin from living cells (J. Lee et al., 2016).

Natural melanin production faces challenges for scale-up due to its cost and limited supply. Moreover, extraction of melanin from bird feathers may introduce contamination, as these sources may contain toxic metals from their ecological exposure. On the other hand, reports suggest that natural melanin outperforms synthetic melanin in biotechnological applications (Tran-Ly et al., 2020).

1.5. Microbial Production

Microbial production of melanin offers several advantages, including the absence of lack of restrictions on seasonal growth, low prices, and environmental friendliness, making microbial melanin a crucial origin of natural melanin. Microbial synthesis involves two pathways with different enzymes. There might be considerable variations in the synthesis of melanin among different microorganisms (Cordero & Casadevall., 2017; Eisenman & Casadevall., 2012; Nosanchuk & Casadevall., 2003; Plonka., 2006; Solano., 2014). The DOPA pathway, also known as DOPA-melanin or eumelanin, transforms tyrosine into L-DOPA, which is further converted to dopaquinone with the assistance of a tyrosinase or laccase. Dopaquinones spontaneously oxidize and polymerize to form melanin. The second pathway, known as the 1,8-dihydroxy naphthalene (DHN) pathway, utilizes malonyl-

coenzyme A as a precursor, producing DHN-melanin through a series of enzymatic reactions (Eisenman & Casadevall., 2012; Pavan et al., 2020;Plonka., 2006). High-yield melanin production is often challenging with microorganisms that use the DHN pathway, as they synthesize melanin endogenously and this tightly binds to the inner side of the cell wall (Toledo et al., 2017). Extraction of melanin from these microorganisms is extremely difficult due to the strong bonding with the cell wall and harsh extraction chemicals lead to artifacts. On the other hand, melanogenesis through the DOPA pathway is considered a mechanism for neutralizing toxic phenolic compounds in the environment (Almeida-Paes et al., 2012; Schmaler-Ripcke et al., 2008). A summary of the melanin synthesis from DHN and DOPA pathways are outlined in Figure 1.4. Many microbes require external tyrosine or tyrosine-derived substrates for melanin synthesis. While tyrosine is the most commonly known substrate, other catecholamines such as dopamine can also be utilized. Melanin production from different substrates can yield structurally diverse melanins because of varied catabolic processes by various enzymes, allowing for the tuning of physicochemical properties and optimization of microbial melanin production.

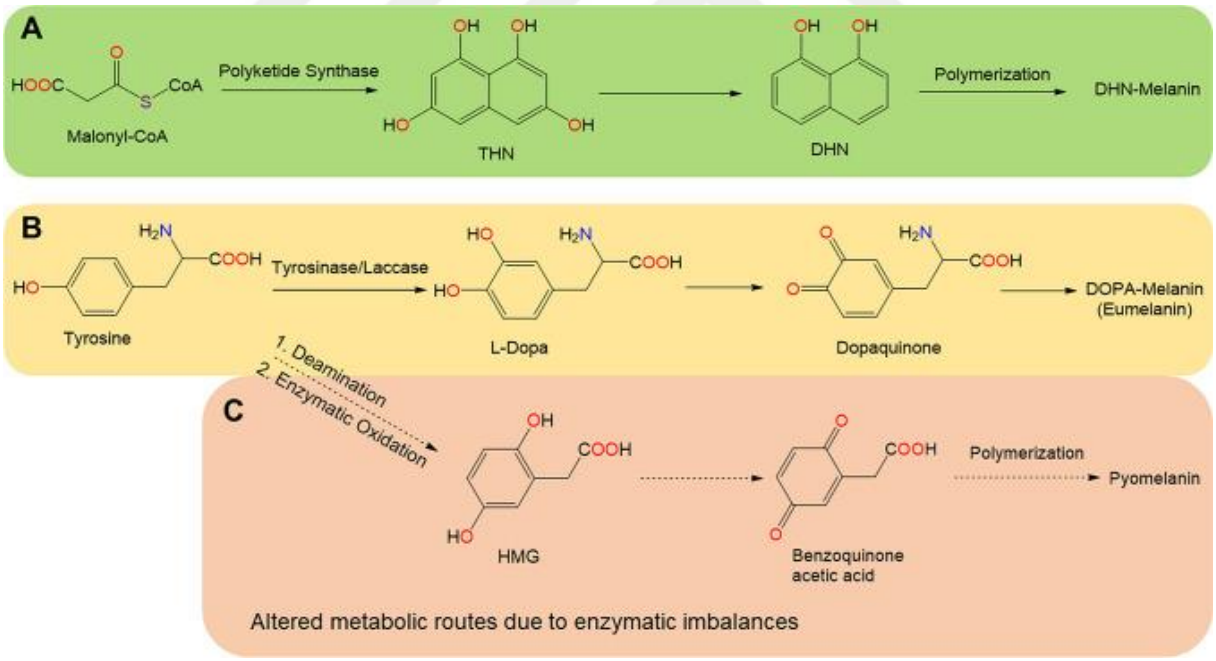

Figure 1.4 The schematic representation that illustrates melanin synthesis, highlighting important chemical transformations shared among microbial melanin-building processes in bacteria and fungi. The pathways depicted include the DHN-pathway (a) and the DOPA-pathway (b). In cases of enzymatic imbalances (c), altered metabolic pathways may result in the formation of different types of melanins, such as pyomelanin (Tran-Ly et al., 2020).

Various factors, including nutritional factors, physicochemical conditions, and the control or modulation of enzymes involved in the synthesis of melanin, significantly impact melanin production. Metals like copper, which serve as cofactors for tyrosinases and laccases, are crucial for melanin production (Reiss et al., 2013; Sendovski et al., 2011; Yang et al., 2017). Different metals, including iron and nickel, can enhance melanin production, although these stress reactions induced in microbes may influence the process of melanin formation (Wang et al., 2018; Gowri., 1996). Other factors such as high temperature, different growth media, and hyperosmotic pressure also support melanin synthesis (Cordero & Casadevall, 2017; Coyne & Al-Harthi., 1992; Fogarty, 1996). Microbial growth and pigment production are influenced by factors like temperature, pH, light, and the presence of oxygen. To this end, statistical tools like the Taguchi method, the Plackett-Burman design, and the Response Surface Methodology maybe utilized to design multifactorial experiments and optimize the impact of each factor in the production process (El- Naggar et al., 2017; Saini & & Melo., 2015; Sun et al., 2016; Surwase et al., 2012). It is clear that a multitude of factors affecting melanin production makes it challenging to identify a specific culture medium or optimum conditions for production by melanogenic microorganisms. Several studies have also explored the use of agricultural residues such as corn steep liquor, wheat bran extract, and fruit waste extract to achieve lower production costs and high-yield production (Hamano & Kilikian., 2006; Silveria et al., 2008; Zou & Tian., 2016).

1.6. Limitations of Microbial Melanin In Commercialization and Industrial Uses

Melanin holds significant potential as a biomaterial, but the commercial use of microbial melanin has been restricted due to its inherent complexity and diversity. The challenges lie in difficult synthetic routes that require maintaining and controlling physical properties, biological functionalities, melanin quality, and performance. The random organization of radicals in melanin contributes to these challenges. Additionally, the economics of melanin production process pose challenges. While materials can produce several grams per liter of end products in industrial applications, economic considerations remain a constraint in the production process. Purification is a further limitation, as it currently involves the use of strong acids/bases and organic solvents, which are not environmentally friendly. There is need to overcome the harsh extraction processes and to adopt to more eco-friendly methods. Finally, commercialization of microbial melanin is also limited by regulations related to human toxicity and concerns about targeting the human body with physiologically active materials, given its production by microorganisms (Choi., 2021).

1.7. Applications of Melanin

Melanin is primarily investigated for its critical role in the virulence of pathogenic organisms, particularly fungi and bacteria (Cordero & Casadevall., 2017). However, advancements in technology have allowed melanin pigments to be repurposed in various fields such as areas of material science, biomedicine, cosmetics, and environmental remediation. One notable physiochemical property of melanin is its innate ability to act as a "natural sunscreen," absorbing the UV-visible light spectrum, making it a potent antioxidant by blocking UV-visible light. Melanin finds major use in hair dyeing and sunscreen for dermal and cosmetic applications. Moreover, it serves environmental purposes as a metal chelator (Figure 1.5).

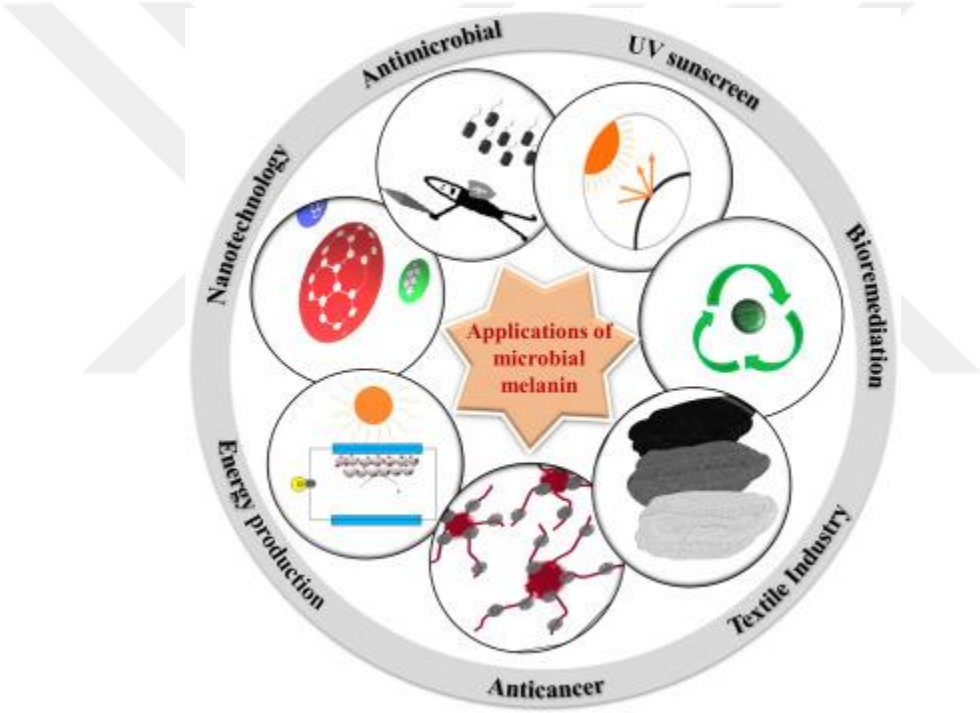

Figure 1.5 Applications of microbial melanin (Singh et al., 2021)

Microbial melanin offers several advantages, including bioavailability, biocompatibility, and biodegradability. In environmental applications, melanin has been employed in the eco-friendly synthesis of silver nanostructures, demonstrating broad-spectrum antimicrobial activity against food pathogens in the food sectors and health sectors (Kiran et al., 2014; Patil et al., 2018).

The co-production of melanin and biochemicals within a single cell holds promise for enhancing melanin's applications in biological processes. Ahn et al. observed the co-production of melanin with important biochemicals, such as cadaverine, a diamino pentane derived from the decarboxylation of lysine (Ahn et al., 2021). Cadaverine is produced directly in relation to melanin polymerization. This co-production strategy not only ensures competitive market pricing but also allows for the simultaneous production of biochemicals through single enzyme expression, adding functionality to the bioprocess (Tran-Ly et al., 2020).

1.8. Melanin Analysis

Pure melanin can be characterized and analyzed by several techniques. Below given is a summary of the techniques that can be used.

It has long been a standard practice to identify and describe the extracted melanin pigments using UV-visible absorption spectra, particularly in the UV range. While this method provides a preliminary understanding, more advanced techniques have been developed to distinguish between different types of melanin or for quantitative goals. Depending on the melanin source, the maximum absorption wavelength for the majority of melanin forms in alkali solutions ranges from 196 to 300 nm. Strong optical absorption in the UV range is exhibited by alkaline melanin solutions, which progressively decrease at longer wavelengths. The complex linked molecules in the melanin structure that absorb, and scatter UV light photons are probably the cause of melanin's significant UV light absorption (El-Naggar & El-Ewasy, 2017; Hou et al., 2019). The subsequent decrease in absorption is nearly linear for most melanins. Consequently, plotting the alkaline melanin solution's logarithm of absorbance against wavelength yields straight lines with negative slopes. These linear plot slopes are frequently employed as essential standards for the detection and description of melanin. One advanced technique commonly used for melanin analysis is Fourier transform infrared spectroscopy (FTIR). FTIR technique is generally advantageous

for accurately assigning spectral characteristics related to functional groups and their corresponding absorption bands, which play important roles in absorption processes (Centeno & Shamir, 2008). Material characterization through FTIR involves creating a spectrum of the radiation energy absorbed by material molecules and interpreting the resulting spectrum. FTIR stands out as a powerful characterization technique due to its speed, non-destructive nature, and the need for small-sized samples. In the material under analysis, chemical bonds vibrate at frequencies specific to their structure, bond angle, and length (Swann & Patwardhan., 2011). These individual molecules can interact with incident radiation by absorbing it at particular wavelengths. By examining individual absorption peaks, one can identify and assign specific chemical bonds, allowing for the qualitative or quantitative identification of individual compounds within complex systems. Scanning Electron Microscopy (SEM) proves to be a robust method for the morphological characterization and determination of particle size distribution in various types of melanins (Mbonyiryivuze et al., 2015; Strube et al., 2015). Numerous sample preparation methods outlined in literature consider factors, such as sample size, shape, state, and conductive properties (Beltrán-García et al., 2014; Büngeler et al., 2017; Prados-Rosales et al., 2015). To achieve conductivity, melanin samples typically need to undergo a coating process. Commonly, a thin layer of gold (Araujo et al., 2012; Costa et al., 2012; Li et al., 2018) or a gold/palladium alloy (Srisuk et al., 2015) is applied for this purpose. The granule morphology of melanin, depending on its source, typical size range of melanin granules usually falls between 30 and 1000 nm, and these granules generally exhibit amorphous characteristics with irregular shapes. Finally, high Performance Liquid Chromatography (HPLC) is an analytical technique that can be used to identify the components alone or in a mixture and separate mixtures of very similar compounds. For the detection of melanin with HPLC, a UV detector is required. The simple sample preparation, sensitivity, and rapidness of HPLC make it advantages over other techniques.

1.9. Metabolic Engineering

Metabolism is a universal process found in all organisms, serving as a central mechanism through which cells harness energy from various sources to generate cellular materials and fulfil energy requirements (Shams Yazdani & Gonzalez, 2008). Strain improvement is paramount for optimizing biotechnological production processes, and metabolic engineering serves as an effective framework for achieving this. Metabolic engineering, pioneered in the early 1990s, represents a revolutionary approach to the rational design of microbial systems

with precisely defined genetics to achieve high production yields (R. R. Kumar & Prasad., 2011). By analysing genome-wide differential gene expression data, along with information on protein substances and in vivo metabolic fluxes, metabolic engineering allows for a comprehensive understanding and manipulation of cellular processes. It operates at the intersection of various multidisciplinary fields, including chemical engineering, biochemistry, and biotechnology. Engineering principles such as the design of metabolic pathways are crucial for achieving targeted goals in this dynamic field (Farmer & Liao, 2000). Metabolic engineering is encouraged by commercial applications where developing methods for improving strains can increase the production of metabolites (F. C. Lee et al., 2010). In the present day, the goals of metabolic engineering are aligned with green chemistry and sustainable development, reflecting the increasing advancements in the biotechnology field, particularly within related industries. The focus on sustainability underscores the broader impact of metabolic engineering in driving environmentally friendly and economically viable processes. In contemporary biotechnology, metabolic engineering is exploited to use renewable plant biomass for the cost-effective production of bulk chemicals (R. R. , & P. S. Kumar, 2011) (Farmer & Liao, 2000)

1.10. *Corynebacterium Glutamicum*

The history of *Corynebacterium glutamicum* as an amino acid producer began with the isolation of *Micrococcus glutamicus* by Kinoshita. In 1956, the company Kyowa Hakko identified it as a natural glutamate producer (Kinoshita et al., 1957; Nakayama et al., 1966; UDAKA., 1960). *Corynebacterium*, a facultatively anaerobic, non-spore-forming gram-positive bacterium, was later renamed *Corynebacterium glutamicum*. It is generally recognized as a safe host (J. Y. Lee et al., 2016) engineered to secrete other amino acids, including L-lysine, L-arginine, L-histidine, and L-valine (Eggeling & Sahm., 1999; Ikeda., 2003; Kimura et al., 2003). Studies on *Corynebacterium* involve the analysis of cell wall composition and lipid sections, highlighting the significance of cell wall chemistry and lipid structure. The cell wall of *C. glutamicum* contains an arabinogalactan polysaccharide partly esterified by mycolic acids, directly cross-linked to peptidoglycan. Additionally, the cell wall features a significant amount of glucose and mannose. Other components include a protein surface layer, high and low molecular mass lipoglycans, arabinomannan, and glucan. *C. glutamicum* boasts several advantages as an industrial host, possessing key physiological properties essential for industrial applications. These properties include: (i) being a safe strain for humans (GRAS); (ii) rapid growth to high cell densities; (iii) genetic stability due

to the lack of a recombination repair system; (iv) a limited restriction-modification system; (v) an extensive spectrum of carbon usages, including hexoses and pentoses; and (vi) robust secondary metabolism. These characteristics make *C. glutamicum* well-suited for cultivation and manipulation in industrial conditions (J. Y. Lee et al., 2016).

1.11. Renewable Carbon Source

The utilization of renewable carbon sources plays a pivotal role in combating climate change by reducing dependence on fossil resources. While decarbonization is a viable strategy in the energy sector, it is not suitable for organic chemistry, which heavily relies on carbon. Thus, it is crucial to explore sustainable and climate-friendly industries that leverage alternative carbon sources, often referred to as renewable carbon. Shifting towards renewable carbon in the chemical industry is imperative given the significance of carbon as a fundamental building block for various applications (Amooghin et al., 2013; Carus et al., 2020). Lignocellulosic biomass, also known as lignocellulose, stands out as one of the most abundant renewable materials globally (Zhou et al., 2011). Produced through the absorption of atmospheric CO_2 and water, using sunlight energy, lignocellulosic biomass consists of phenolic polymers, polysaccharides, and proteins. Its complex spatial structure involves cellulose, hemicellulose, and lignin. Cellulose, a carbohydrate polymer, is enveloped by a dense structure formed by hemicellulose, other carbohydrate polymers, and lignin, an aromatic polymer. Lignocellulosic biomass generally exists in three forms: biomass, virgin biomass, and energy crops (Yousuf et al., 2019).

1.11.1. Orange peel hydrolysate

Production of oranges is generally increasing each year, and within the orange industry, orange peel is recognized as the garbage with both the highest volume and the greatest potential benefit. It is estimated that orange peel constitutes approximately 20% of an orange. According to literature findings, orange peel comprises 11% hemicellulose, 22% cellulose, 23% sugar, and 25% pectin. The utilization of orange peel as a carbon source is of significant interest. Establishing an integrated process that effectively converts the hemicellulose content of the biomass into fermentable sugars, is essential for microbial utilization. This conversion process ensures easy accessibility for microorganisms during fermentation. The carbohydrate monomers obtained from the degradation of polymers include glucose, fructose, xylose, and galactose. Among the processes used to achieve this

degradation are acid hydrolysis, fermentation, and enzymatic hydrolysis. For orange peel, one easy and economical method for hemicellulose and cellulose degradation is hydrolysis with diluted acid, as demonstrated by Ayala et al. (2021). This approach is considered the suitable option for breaking down the complex components of orange peel into simpler sugars, facilitating subsequent processes such as fermentation (Ayala et al., 2021).

1.12. Model Based Optimization

Numerical optimization entails the use of mathematical models to identify values for decision factors (independent variables) that either minimize or maximize an objective function (dependent variable or response). Different numerical optimization methods are employed based on the arrangement of the mathematical model and characteristics of the target function. In this study, conditions for highest melanin titers have been found via global optimization using Kriging and Quadratic methods. In this research, global optimization was employed, aiming to identify the optimal values of variables for obtaining highest melanin titers. Given the potential presence of multiple local optima, the goal of global optimization is to pinpoint the global optimum of the system (Brownlee, 2021). In this study, both low-order polynomials (frequently used for RSM) and Kriging methods were used for modelling and optimization.

2. MATERIALS AND METHODS

2.1. Materials

2.1.1. Strains

The strains used in this study are summarized in Table 2.1.

Table 2.1 List of strains and descriptions

Strain	Description	Reference
EKV-I	*C. glutamicum* ATCC 13032 harbouring pEKEx2-tyr_{Rs}	(Kurpejović et al. 2021)
EKV-II	EKV-I harbouring pEKEx3-$xylA_{Xc}$-$xylB_{Cg}$	(Kurpejović et al. 2021)
AROM3D	AROM3 harbouring pEKEx3-tyr_{Rs}	(Kurpejović et al. 2023)

2.1.2. Chemicals

D(+)-glucose was from NeoFroxx, IPTG (Isopropyl β-Dithiogalactopyranoside) was from BioFroxx, MOPS (3-morpholinopropanesulfonic acid) was from Wisent, brain heart infusion (BHI) was from Biolife, L-tyrosine was from Multicell, Ammonium sulfate, kanamycin sulfate, urea, manganese (II) sulfate monohydrate, glycerol, Biotin were from Sigma, Spectinomycin dihydrochloride 5-hydrate was from AppliChem, 3,4-Dihydroxybenzoic acid, protocatechuic acid (PKS) were from Alfa Aesar, and Agar, sodium chloride, calcium chloride, and nickel (II) chloride hexahydrate, magnesium sulfate heptahydrate, copper (II) sulfate pentahydrate, di-potassium hydrogen phosphate were from Merck, and potassium phosphate monobasic, iron (II) sulfate heptahydrate, zinc sulfate heptahydrate were from Isolab.

2.1.3. Buffers and media

Brian-Heart infusion medium: Firstly, 37 g of BHI were weighed and dissolved in 1 liter of distilled water. It was autoclaved for 15 minutes at 121 degrees Celsius. 15 g of agar were weighed for 1 liter of BHI medium for growth experiments to prepare a solid medium. After autoclaving, the mixture was poured onto petri dishes.

CgXII defined medium: CgXII medium was prepared by mixing 900 mL of basic medium and 100 mL of a solution with the carbon source. The basic medium had 5 g/L urea, 1 g/L K_2HPO_4, 1 g/L KH_2PO_4, 20 g/L $(NH_2)_2SO_4$, and 42 g/L MOPS. The pH of the basic medium was adjusted to 7 with 10 M NaOH. 40% glucose solution was used as the carbon source. The final concentration of glucose in the CgXII medium was 4%. The two components were autoclaved at 121 degrees Celsius for 15 minutes. For Cg-EKV-I, CgXII defined medium was supplemented with 1 g/L L-Tyr.

CgXII medium with orange peel hydrolysate as the carbon source: When orange peel hydrolysate was used as the main carbon source, 5X basic CGXII medium was prepared as a concentrated solution. This medium was prepared by dissolving 100 g/L $(NH_2)_2SO_4$, 25 g/L urea, 5 g/L KH_2PO_4, 5 g/L K_2HPO_4, and 210 g/L MOPS in 1 liter of distilled water. The medium with orange peel was autoclaved at 121 degrees Celsius for 15 minutes. The pH of the orange peel hydrolysate was then adjusted to 7 using 10 M NaOH. The medium was prepared by mixing 80 ml hydrolysate with 20 ml 5X concentrated basic medium.

Trace elements: For 1 Liter of CgXII medium 0.25 g/L $MgSO_4.7H_2O$, 10 mg/L $CaCl_2$, 10 mg/L $MnSO_4.H_2O$, 10 mg/L $FeSO_4.7H_2O$, 1 mg/L $ZnSO_4.7H_2O$, 0.2 mg/L $CuSO_4.5H_2O$, 0.02 mg/L $NiCl_2.6H_2O$, 0.2 mg/L biotin, and 30 mg/L protocatechuic acid were prepared and sterilized using 0.22 um filters. They are kept at -20 degrees Celsius. The trace elements were mixed with a basic medium and carbon source before cultivation started.

Acid treatment of orange peel: Orange peels were dried in an oven at 75 °C for 2 days and then blended into a powder form. 12.5 g of orange peel were weighed and mixed with 2% H_2SO_4 in 100 mL of distilled water. Afterwards, the mixture was autoclaved at 121 degrees Celsius for 50 minutes. The orange peel was filtered using filter paper after autoclaving. Approximately 50-60 mL of the filtered orange extract was then adjusted to pH 7 with 10 M NaOH. The hydrolysate was sterilized for 15 minutes at 121 degrees Celsius to be used in growth media.

The formulations of all media and used all buffers are presented in Table 2.2.

Table 2.2 List of media and buffers used.

Media and buffers	**Composition**
Brain heart infusion media (BHI)	37 g/L BHI
Brain heart infusion agar plates	15 g/L agar 37 g/L BHI
CGXII minimal medium Trace element solution's:	20 g/L $(NH_2)_2SO4$, 5 g/L urea, 1 g/L KH_2PO_4 1 g/L K_2HPO_4 42 g/L MOPS 4% (w/v) glucose 0.25 g/L $MgSO_4 \cdot 7H_2O$ 10 mg/L $CaCl_2$ 10 mg/L $FeSO_4 \cdot 7H2O$ 10 mg/L $MnSO_4 \cdot H2O$ 1 mg/L $ZnSO_4 \cdot 7H2O$ 0.2 mg/L $CuSO_4 \cdot 5H_2O$ 0.02 mg/L $NiCl_2 \cdot 6H_2O$ 0.2 mg/L biotin 30 g/L protocatechuic acid (PKS)

2.2. Methods

2.2.1. Experimental techniques

2.2.1.1. Cultivation conditions

All strains were kept in 25% glycerol solution at -80 °C. *C. glutamicum* strains were cultured in 25 mL and 50 mL CGXII medium in 250 mL and 500 mL baffled flasks. The strains were grown under the following conditions:

Glycerol stocks were retrieved from the freezer and streaked onto BHI agar plates. Subsequently, the plates were incubated for two days at 30 °C. A single colony from each

plate was selected and inoculated into 5 mL BHI medium for 8 hours and 200 rpm at 30 °C. For Cg-EKV-I, 25 μg/mL of kanamycin was supplemented to the medium, for AROM3D, 100 μg/mL of spectinomycin was supplemented, and both antibiotics were added for Cg-EKV-II.

50 mL of CGXII medium with a 4 % carbon source was inoculated with 1 mL of the overnight preculture, adjusting the OD_{600} to 1 for the main culture (Keilhauer et al., 1993). This mixture was cultivated in 500 mL flasks overnight 150 rpm and at 30 °C for a total of 18 hours, serving as the preculture.

2.2.1.2. Fermentative melanin production with Cg-EKV-I

The Cg-EKV-I strain harboring pEKEx2-tyr_{Rs} was employed for melanin production using glucose as the sole carbon source. An overday culture of a single colony was incubated in 5 mL BHI tubes with kanamycin at 30 °C and 200 rpm in a shaker for 6-8 hours. The second preculture was prepared by mixing 25 mL of CgXII basic medium supplemented with trace elements, kanamycin, and 4 % (w/v) glucose and inoculated with 1 mL of the overday culture in a 25 mL flask. The flask was placed in a shaker at 30 degrees Celsius, 150 rpm for 16-18 hours. The production medium was 50 mL of CgXII medium supplemented with L-Tyr, glucose, trace elements, and kanamycin. Additionally, 0.1-0.6 mM $CuSO_4$ was added to activate the tyrosinase enzyme. The production medium was inoculated with the second preculture adjusting the initial OD_{600} to 1. The flask was incubated at 30 °C, 150 rpm. After 90 minutes, 1 mM of IPTG was added as the inducer. Cells were grown up to 144 hours. Growth was monitored by measuring OD_{600} value. To get the final value the OD_{600} value of the cell-free culture was subtracted from the OD_{600} of the culture-containing cells. This resulting value was then converted to dry cell weight per milliliter using a calibration curve. The cell-free supernatant was analysed for melanin and L-Tyr production. To study if L-Tyr amount limited melanin formation, additional L-Tyr was added in powder form after 24 hours to get a final concentration of 4 g/L and melanin formation was followed.

2.2.1.3. Fermentative melanin production with AROM3D

The AROM3D strain was utilized for melanin production from glucose as the sole carbon source. An overnight production culture was prepared from a single colony on a BHI plate with spectinomycin. The single colony was incubated in 5 mL BHI tubes with spectinomycin at 30 °C and 200 rpm in a shaker for 6-8 hours. The second preculture was prepared by mixing 25 mL of CgXII basic medium supplemented with trace elements, spectinomycin, and 4 % (w/v) glucose and inoculated with 1 mL of the overday culture in a 25 mL flask. Additionally medium was supplemented with 2 mM L-Phe, and 1 mL since the strain is a L-Phe bradytrophs. The flask was placed in a shaker at 30 degrees Celsius, 150 rpm for 16-18 hours. The production medium was 50 mL of CgXII medium supplemented with glucose, trace elements, spectinomycin, and 0.5 mM L-Phe. Additionally, 0.1 mM $CuSO_4$ was added to activate the tyrosinase enzyme. The production medium was inoculated with the second preculture adjusting the initial OD_{600} to 1. The flask was incubated at 30 °C, 150 rpm. After 90 minutes, 1 mM of IPTG was added as the inducer. Cells were grown up to 144 hours, growth was monitored by measuring OD_{600} value. To get the final value the OD_{600} value of the cell-free culture was subtracted from the OD_{600} of the culture-containing cells. This resulting value was then converted to dry cell weight per milliliter using a calibration curve. The cell-free supernatant was analysed for melanin and L-Tyr production. To study if L-Tyr amount limited melanin formation, additional L-Tyr was added in powder form after 24 hours to get a final concentration of 4 g/L and melanin formation was followed.

2.2.1.4. Melanin production from orange peels sugar extract in Cg-EKV-II

When orange peel hydrolysate was used for melanin production, the overnight preculture medium contained 20 % (v/v) orange peel hydrolysate and LB medium. When essential, 25 µg/mL kanamycin and 100 µg/mL spectinomycin were supplemented. The preculture was grown at 30 °C, 150 rpm, for 16-18 hours. The grown cells were harvested, washed with CgXII medium without glucose, and used to inoculate the main culture. The main culture consisted of 30 % orange peel hydrolysate., and the cells were grown at shaker 150 rpm at 30 °C for 48 hours. Based on the mathematical optimization results 0.31 mM copper ions wer added as a cofactor for the enzyme . After 90 minutes, 1 mM of IPTG was added as the inducer. Growth was monitored by measuring OD_{600} value. To get the final value the OD_{600} value of the cell-free culture was subtracted from the OD_{600} of the culture-containing cells. This resulting value was then converted to dry cell weight per milliliter using a calibration

curve. Cells were grown for 48 hours, and the cell-free supernatant was analysed for melanin production.

2.3. Melanin Extraction

Grown cells were centrifuged at 2600 g for 15 minutes to separate and obtain the cell free supernatants with melanin. The resulting supernatant was acidified using 3 molar HCl to achieve a pH of 3. The acidified sample was then incubated in an oven at 30°C for 24 hours. Subsequently, the sample was centrifuged at 2600 g for 15 minutes to obtain crude melanin pigments. The melanin pellet was washed with a 1:1 ratio of acetone and ethanol. The pigments, mixed with acetone-ethanol, were centrifuged at 2600 g for 15 minutes, and the supernatant was discarded. Finally, the precipitated pigments, containing melanonids, were boiled in a water bath for 15 minutes to eliminate the melanoidins. The obtained pigments were dried in an oven at 50°C for 3 days (Gibson & George, 1998; Eskandari & Etemadifar, 2021). Melanin was resuspended in 0.5 M NaOH for further characterization.

2.4. Melanin Quantification

Eumelanin determination was carried out in the cell-free supernatants at OD_{400} nm following the method described by Turick et al. (2002) (Turick et al., 2002). The obtained OD_{400} value was then converted to melanin titer using the conversion factor of 0.066 g/L = 1 OD_{400}, as reported by Ahn et al. (2021) (Ahn et al., 2021). Subsequently, this value was converted to dry cell weight per milliliter using a calibration curve. The entire cell-free culture was stored at +4°C for further analyses (Lagunas-Munoz, 2006).

2.5. Analysis of melanin with High Performance Liquid Chromatography

High-Performance Liquid Chromatography (HPLC) analysis was performed using the Agilent 1100 system, equipped with a C18 Zorbax column (250 × 4.6 mm, 5 µm), and a UV detector set at 280 nm. A mobile phase comprising methanol and 1% acetic acid in a 20:80 ratio was used. The flow rate was fixed to 0.5 mL/minute, and the running time was set at 20 minutes. An injection volume of 20 µL for melanin dissolved in 0.5 M NaOH was utilized. The temperature was maintained at 50 °C (Sun et al. 2016) (Eskandari & Etemadifar., 2021). The HPLC chromatogram of the purified melanin was compared to that of the standard melanin from *Sepia officinalis* (Sigma CAS no: 8049-97-6) (Sigma M2649).

2.6. Analysis of L-tyr High Performance Liquid Chromatography

To monitor L-Tyr consumption as the substrate during melanin production, HPLC was employed. As recently described by Kurpejović et al. (2023), an Agilent 1100 system equipped with a C18 Zorbax column (250x4.6 mmx5µm) and a UV detector set at 280 nm was utilized (Kurpejović et al., 2023). The mobile phase consisted of 0.1 N acetic acid-methanol at a ratio of 10:1. The flow rate was set to 1.2 mL/min, and the analysis was carried out at 30°C. An injection volume of 20 µL was used for each sample. The retention time for standard L-Tyr was determined to be 3.3 minutes.

2.7. Analysis of melanin with UV-Vis Spectrophotometry

Dilutions of the extracted melanin, dissolved in 0.5 M NaOH, were prepared in double-distilled water at ratios of 1:10 and 1:100. The pH of the solutions was adjusted to 12 using 1 N NaOH. Different concentrations of the purified melanin (0.1, 0.125, 0.05, 0.25 g/L) were then prepared using these dilutions. Alkaline double-distilled water adjusted to pH 12 served as the blank. The solutions were scanned at UV and visible wavelengths (200-900 nm) using a spectrophotometer (Bio-Rad, Smart Spec Plus). The relationships between log absorbance and wavelength were calculated and plotted according to the method described by Raman and Ramasamy (Raman & Ramasamy., 2017).

2.8. Analysis of melanin with Fourier Transform Infrared Microscopy (FT/IR)

The functional groups and bond structures of the purified melanin were identified using a Fourier Transform Infrared spectrophotometer (FTIR, Jasco FT/IR-4700). The instrument was provided with a Gladi Attenuated Total Reflection (ATR) viewing plate (Diamond ATR crystal) and a liquid-nitrogen-cooled mercury cadmium telluride (MCT) detector. Spectra were recorded in the wavelength range of 4000 cm^{-1} to 400 cm^{-1} at a temperature of 23°C (Mahmutoglu et al., 2023).

2.9. Analysis of melanin with scanning electron microscopy (SEM)

For SEM analysis, melanin was fixed on membranes following the procedure previously described by Gokgoz (Gokgoz., 2017). Specifically, 25 µL of a melanin solution in 0.5 M NaOH, containing approximately 20 mg of purified melanin, was carefully deposited onto a 0.22 µm pore sized membrane filter. The samples were then fixed for 90 minutes by floating the filters on 2% glutaraldehyde. After fixation, the samples were washed with distilled water. The filters were dehydrated by sequential immersion in increasing concentrations of

ethanol (30%, 50%, 70%, and 90%) for 10 minutes each, followed by immersion in absolute ethanol for 1 hour. Subsequently, the filter was air-dried overnight at room temperature and coated with platinum using a sputter coater before imaging. Imaging was performed using a Philips XL30 ESEM-FEG/EDAX system under high vacuum mode, with 5 kV energy and a 3.0 spot size.

2.10. Whole cell biocatalysts with orange peel hydrolysate

The CgEKV-II strain was grown on 30% orange peel hydrolysate for 48 hours. At the end of this period, the cells were centrifuged at 10.000 g for 10 minutes. The supernatant was discarded, and the cells were collected. The cells were then resuspended in water to achieve a calculated OD_{600} of 1. A solution of 1 g/L L-Tyr was prepared using distilled water. In 15 mL falcon tubes, 10 mL of the prepared L-Tyr solution was mixed with CgEKV-II cells with varying volumes from 50 µL to 450 µL. A total of 18 different conditions were conducted for melanin production. The experiments were conducted under two sets of conditions: the first set was without shaking at room temperature, and the second set was at 150 rpm in a shaker at 30 °C. To each falcon tube, 100 µL of copper ions were added to activate the tyrosinase. After 24 hours, the tubes were centrifuged at 10.000 rpm for 10 minutes, and the OD_{400} of the samples was measured using a spectrophotometer.

2.11. Model based optimization

2.11.1. Design of experiments

Two sets of data points were selected to design experiments with three independent variables (factors): copper addition time, copper concentration, and L-Phe concentration. The limits for the variables were: 0-24 hours for copper addition, 0-0.4 mM for copper ion concentration, and 0-0.5 mM for L-Phe concentration. The first set of data points were designed using a traditional approach. 12 data points were randomly selected using MATLAB's function. Experiments with these data points were tested in triplicate. The second set of data points were selected with 3 factors and 5 levels using MATLAB's ccdesign to support the modelling. Here, the total number of experiments was 24 with 10 center points. 10 repetitions allowed for a more uniform estimation of prediction variance.

2.11.2. Modelling and optimization

Two approaches were used to model the experimental data and determine the optimum values of the selected independent variables. These were low-order polynomial modelling, which is often used as a part of response surface methodology (RSM) and Kriging. For RSM (low-order polynomial), MATLAB's fitlm function has been used. The response (dependent variable) was melanin titer. For Kriging, MATLAB's fitrgp function has been used. This is a quadratic model and has a pure quadratic basis function and a rational quadratic kernel function. In both modeling approaches, for a comprehensive description of the model, all data were used were used to fit a model. Then for numerical optimization, MATLAB's global optimization toolbox was utilized. Unlike general optimization toolbox solvers, the global optimization toolbox is specifically designed to explore multiple local minima. The primary improvement value utilized was fmincon, employing the interior point algorithm for minimization under constraints. The fmincon function is tailored for identifying the minimal of nonlinear and multiple variable functions. The optimal values for the concentration of copper ions, copper addition time, and L-Phe concentration were determined for maximum melanin titer.

3. RESULTS AND DISCUSSION

3.1. Melanin production with Cg-EKV-I

Tyrosinases function as copper-dependent enzymes, catalyze the hydroxylation of L-Tyr to L-DOPA. These enzymes, while primarily focused on L-Tyr conversion, also possess bifunctionality, converting L-DOPA to L-dopaquinone, which is subsequently oxidized to form melanin (Valıpour., 2015). To this end, CgEKV-I cells, engineered for the conversion of L-Tyr to L-DOPA as outlined by Kurpejović et al. (Kurpejović et al. 2021), were employed for melanin synthesis using externally supplemented L-Tyr. Initially, for melanin production with these cells, an optimal concentration of 0.4 mM copper ions was established for L-DOPA production (Kurpejović et al., 2021).

3.1.1. Effect of different copper ion concentrations

Since tyrosinase is activated by the presence of copper ions, melanin production was investigated with different copper ion concentrations ranging from 0.1 to 0.6 mM with Cg-EKV-I for 72 hours. It can be inferred that concentrations above 0.3 mM of copper ions exhibited a toxic effect on melanin production, as indicated by lower melanin yields and lower cell yields. The results are given in Table 3.1.

Table 3.1 Effect of different copper ion concentrations for Cg-EKV-I

Time (hour)	0.1 mM	0.2 mM	0.25 mM	0.3 mM	0.4 mM	0.6 mM
24	0.51±0.1	0.59±0.1	0.84±0.1	0.85±0.1	0.67±0.3	0.44±0.1
48	0.75±0.1	0.81±0.1	0.91±0.1	0.93±0.04	0.75±0.1	0.52±0.1
72	0.81±0.1	0.84±0.1	0.93±0.04	0.95±0.04	0.78±0.1	0.57±0.1

The highest melanin production was with 0.3 mM copper ions after 24, 48, and 72 hours. Overall, production with 0.25 mM and 0.3 mM copper yielded very similar melanin titers. Based on the results in Table 3.1, production with 0.1 mM and 0.2 mM copper ions yielded similar melanin titers. Although melanin titer with 0.1 mM copper ions was lower than the titerl obtained with 0.3 mM copper ions, considering environmental issues, this concentration could also be considered for melanin production with this system and production period could be 72 hours. There was only a slight difference (10-15%) in melanin

titer with low copper ion concentrations. Therefore, further experiments with Cg-EKV-I were completed in the presence of 0.1- or 0.2-mM copper ions.

3.1.2. Effect of different flask volumes

Different production volumes were considered since they directly influence oxygen availability and consequently L-DOPA oxidation to form melanin. To this end, growth media as 25, 50, and 75 mL in 500 mL flasks for melanin production with Cg-EKV-I have been considered and the obtained results are displayed in Table 3.2. Among the production volumes tested, the lowest melanin production was in 75 mL with 0.84 g/L melanin after 72 hours, probably due to oxygen insufficiency. Although production in 25 mL seemed slightly better, due to excessive foaming, it was difficult to work with this volume. Therefore, optimum production volume was selected as 50 mL for further experiments.

Table 3.2 Effect of culture volume on melanin production with Cg-EKV-I.

Time	Melanin titer (g/L)		
	25 mL	**50 mL**	**75 mL**
24	0.54±1.0	0.82±0.4	0.40±0.2
48	0.94±0.03	0.85±0.02	0.65±0.2
72	0.97±0.03	0.90±0.03	0.84±0.04

3.1.3. Effect of different rotation speeds

Under rigorous shaking, oxygen transfer rate increases, therefore different rotation speeds of the shake flasks during cultivation were considered. Melanin production was again achieved in 500 mL flasks with 50 mL growth media. Tyrosinase was activated with 0.1 or 0.2-mM copper ion (Table 3.2). Production was followed for 72 hours. The three different speeds tested were 120, 150, and 200 rpm. With 0.1 mM copper ions, the lowest production was with 120 rpm for which the maximum titer was 0.58 g/L after 48 hours (Table 3.3). The highest production was with 200 rpm for which the titer was 0.89 g/L. The titer with 150 rpm as 0.81 g/L was very close to the titer obtained with 200 rpm.

Table 3.3 Effect of rotation speed on melanin production by Cg-EKV-I with 0.1 mM copper ions

Time	Melanin titer (g/L)		
	120 rpm	**150 rpm**	**200 rpm**
24	0.35	0.59	0.65
48	0.58	0.81	0.89
72	0.58	0.81	0.89

Melanin titers obtained when copper ion concentration was 0.2 mM are given in Table 3.4. Again, the three different rotation speeds used were 120, 150, and 200 rpm. Interestingly, the lowest production which was with 200 rpm and the titer after 48 hours was only 0.45 g/L. The highest production was with 150 rpm and the titer was 0.75 g/L.

Table 3.4 0.2 mM copper concentration at 120, 150, and 200 rpm with Cg-EKV-I on melanin production

Time	Melanin titer (g/L)		
	120 rpm	**150 rpm**	**200 rpm**
24	0.35	0.59	0.40
48	0.55	0.75	0.45
72	0.58	0.75	0.45

Considering 0.1 mM copper ion concentrations, 200 rpm was the best but when energy consumption issues are considered, 150 rpm could be regarded feasible. Furthermore, foaming with higher rotations was unfavorable. Considering 0.2 copper ion concentrations, 150 rpm was the best. In either case, 120 rpm was not enough for high production. So, 150 rpm selected for further work.

3.1.4. Effect of different additional L-Tyr

In order to increase melanin titer, the medium was supplemented with additional L-Tyr. In the first attempt, after 24 hours L-Tyr was added to get a final concentration of 4 g/L g. For this, three different L-Tyr addition times were tested to enhance melanin production. Additions were achieved in powder form melanin since the low solubility of L-Tyr prevented

concentrated stock preparation. All the samples contain 0.1 mM copper. Titers and yields were calculated from 24 to 144 hours. The yield on L-Tyr calculated are given in Table 3.5.

However, there was no significant difference observed between the control group and the group with an additional 0.2 g of L-Tyr for melanin production. When compared to three different conditions, the lowest melanin production was with the addition of L-Tyr after 48 hours. Additionally, neither the addition of 0.1 g of L-Tyr after 24 hours nor after 48 hours efficiently produced melanin. It can be inferred that L-Tyr cannot be effectively utilized after 48 hours, as the titer was calculated to be very low. There was a notable difference between the addition of 0.2 g of L-Tyr after 24 hours and the addition of 0.1 g of L-Tyr after both 24 and 48 hours. (Lagunas-Munoz. 2006).

Table 3.5 Effect of additional 4 g/L L-Tyr supplement at different times for melanin production by CgEKV-I (yield on L-Tyr).

Time (hour)	**Control**	**4 g/L L-tyr added, @ t_{24}**	**4 g/L L-tyr added, @ t_{48}**	**2 g/L L-tyr added, @ t_{24}, 2 g/L L-tyr added, @ t_{48}**
24	0.24	0.36	0.18	0.36
48	0.80	0.23	0.57	0.34
72	0.92	0.23	0.12	0.20
96	0.69	0.32	0.12	0.29
120	0.87	0.33	0.13	0.32
144	0.93	0.33	0.13	0.32

If we compare with the control, there was no huge difference with additional L-Tyr. Melanin titer was higher but yield on L-Tyr was not higher. Therefore, it was not feasible to add extra L-Tyr.

3.1.5. Effect of flask geometry

Finally, melanin production in flasks with different geometries was investigated. Again after 48 hours there was no significant melanin accumulation. In the first 24 hours melanin accumulation was higher in the flask with larger baffles and closed with tin cotton. This

could be because exposure to oxygen was slightly higher, e.g. aeration rate could be higher. Thus L-Tyr is converted to melanin faster. However, after that time, the titers were pretty similar in the two different flasks (Table 3.6).

Table 3.6 Effect of different flask geometries for Cg-EKV-I

Time (hour)	Titer (g/L)	
	Flask with larger baffles and closed with tin cotton	**Flask with larger baffles and closed with a blue cap**
24	0.29	0.16
48	0.69	0.65
72	0.65	0.71

3.1.6. Summary with CgEKV-I cells

Under the conditions determined for L-DOPA production, in the absence of the antioxidant, L-DOPA was expected to be converted to melanin. Following a 24-hour production period, melanin titer with CgEKV-I cells reached 0.67±0.4 g/L. There a was a subsequent increase to 0.75±0.1 g/L after additional 24 hours. Extended production times beyond this point resulted in only marginal improvements in titer (72 hours: 0.78±0.1 g/L and 96 hours: 0.82±0.1). Consequently, for further optimization experiments involving externally added L-Tyr, the selected production time was set at 48 hours. In the work by Kraseasintra et al. (Kraseasintra., 2023), cultivation was for 7 days at 150 rpm and at 30 °C. The time required in study took much longer compared to our work, and despite the extended duration, produced melanin titer was lower. In the work by Elsayis (Elsayis., 2022), melanin was produced with 2 g/L of tyrosine addition, and the production medium consisted of beef extract peptone. On the other hand, in this thesis, rather than a rich medium, defined medium was used. This was favourable for scale-up and industrial production. Additionally, only 1 g/L L-tyr was used for melanin production. Furthermore, their incubation period was 10 days at 30 °C with an agitation speed of 180 rpm. They have reported a maximum melanin yield of 0.938 g/L (Elsayis., 2022). In this study, melanin was obtained without using a simpler medium and the production time was only 2 days, at 30 °C with agitation speed 150 rpm. The maximum melanin yield was approximately 0.91 g/L.

3.2. Melanin production with AROM3D

Copper ions play a crucial role in tyrosinase activity; however, their presence significantly hampers AROM3D growth (published data). Beyond their impact on microbial growth, copper ions raise environmental and sustainability concerns. The release of copper ions into the environment can induce toxicity in aquatic ecosystems and soil, posing risks to non-target organisms. Moreover, copper mining and extraction processes carry substantial environmental consequences, including habitat destruction and water pollution. In comparison to alternative methods that employ more environmentally friendly materials, copper-based microbial production processes exhibit a less sustainable overall lifecycle. In light of these considerations, a preliminary optimization of copper ions was conducted by externally adding L-Tyr as a proof-of-concept study. The presence of $CuSO_4$ in the medium was found to enhance melanin production by increasing enzymatic activity; however, excessive $CuSO_4$ concentration could exert toxicity on cells, leading to a reduction in melanin yield (Plonka., 2006). In the findings of Zou and Hou (2017), indicate that L-tyrosine can enhance melanin production, but an excess of L-Tyr may have a counterproductive effect. This is attributed to the reduced solubility of L-Tyr at higher concentrations, leading to substrate accumulation in the reactor through precipitation. The accumulation can disrupt normal cell functioning, as the degradation of L-Tyr releases ammonia. So, in the second part of the study, melanin was produced without external L-Tyr (Kraseasintra., 2023).

3.2.1. Effect of copper addition time and L-Phe concentration

AROM3D cells are L-Phe bradytroph, therefore L-Phe supplementation was necessary. On the other hand, high L-Phe concentrations inhibit L-Phe synthesis. To this end, 0.25- and 0.5-mM L-Phe concentrations were tested with initial 0.1 mM copper addition and 0.1 mM copper addition after 24 hours. The results are given in Table 3.7. Here, if copper is added after 24 hours, melanin production is not efficient, indicating that it should be added earlier in the process. In the initial stages of the experiment, copper ions were introduced. Upon considering L-Phe concentrations ranging between 0.25 mM and 0.5 mM, it was observed that a concentration of 0.5 mM of L-Phe yielded better results compared to 0.25 mM concentrations.

Table 3.7 Melanin production with 0.25 or 0.5 L-Phe and 0.1 mM copper at t_0 and t_{24}

Melanin (g/L)

Time	0.5 mM L-Phe, copper @ t_0	0.25 mM L-Phe copper @ t_0	0.5 mM L-Phe copper @ t_{24}	0.25 mM L-Phe copper @ t_{24}
24	0.39	0.32	0.07	0.18
48	0.51	0.46	0.16	0.19
72	0.49	0.55	0.23	0.26

3.2.2. Effect of copper and L-Phe concentration on melanin production

Three different copper and L-Phe concentrations were tested for optimum melanin production. Results are given in Tables 3.8, 3.9, and 3.10. When comparing 0.1 mM, 0.2 mM, and 0.3 mM copper ions, it was found that 0.2 mM and 0.3 mM copper ions resulted in nearly identical melanin production levels, suggesting that 0.2 mM was preferable over 0.3 mM copper ions. Upon comparing 0.2 mM and 0.1 mM copper ions, the difference between them was not significant, indicating that 0.1 mM copper ion was the optimal concentration. Similarly, when considering L-Phe concentrations of 0.125 mM, 0.25 mM, and 0.50 mM, 0.50 mM was determined to be the optimal concentration due to its efficiency in melanin production.

Table 3.8 0.1 mM copper ion and 0.125, 0.25, 0.50 mM L-Phe concentrations were added initially with AROM3D on melanin production.

Time	0.125 L-Phe (mM)	0.25 L-Phe (mM)	0.5 L-Phe (mM)
24	0.16	0.27	0.39
48	0.25	0.40	0.50
72	0.27	0.43	0.43

Table 3.9 0.2 mM copper ions and 0.125, 0.25, 0.50 mM L-Phe concentrations were added initially with AROM3D on melanin production.

Time	0.125 L-Phe (mM)	0.25 L-Phe (mM)	0.5 L-Phe (mM)
24	0.13	0.22	0.33
48	0.30	0.49	0.67
72	0.30	0.65	0.67

Table 3.10 0.3 mM copper ions and 0.125, 0.25, 0.50 mM L-Phe concentrations were added initially with AROM3D on melanin production.

Time	0.125 L-Phe (mM)	0.25 L-Phe (mM)	0.5 L-Phe (mM)
24	0.12	0.12	0.15
48	0.22	0.46	0.69
72	0.35	0.57	0.79

3.2.3. Growth curve analysis with dissolved oxygen measurement

After determining the optimal conditions for melanin production with an initial addition of 0.1 mM copper ions and 0.5 mM L-Phe concentration, the growth curve of this production was analysed. To facilitate comparison, production under the same conditions but with copper ions added 24 hours later was also assessed. The growth graph was generated based on dissolved oxygen data collected over a 72-hour period using the growth curve. The observation of growth cessation at 72 hours indicates that these production processes can endure for up to 72 hours.

According to Figure 3.1, specific production conditions were selected, and changes in oxygen levels were observed using AROM3D strains with the growth curve. Two different conditions were tested in the experiment. The first production, depicted by the dot commenced with an initial addition of 0.5 mM L-Phe and 0.1 mM Cu. The second production, illustrated by the triangle, began with an initial addition of 0.5 mM L-Phe, followed by the addition of 0.1 mM Cu after 24 hours. Both productions started with the same initial oxygen level of 85. Notably, the second production exhibited faster growth compared to the first production. The first production sustained growth until 36 hours, as

evidenced by the increase in oxygen levels after 36 hours. Similarly, the second production displayed growth until 30 hours, as indicated by the rise in oxygen levels after 30 hours. By the 50-hour mark, both productions entered the death phase. Despite the time difference, the first production demonstrated greater efficacy than the second production in terms of melanin production. The cells continued to grow up to 72 hours, suggesting that the optimal production time extends up to 72 hours.

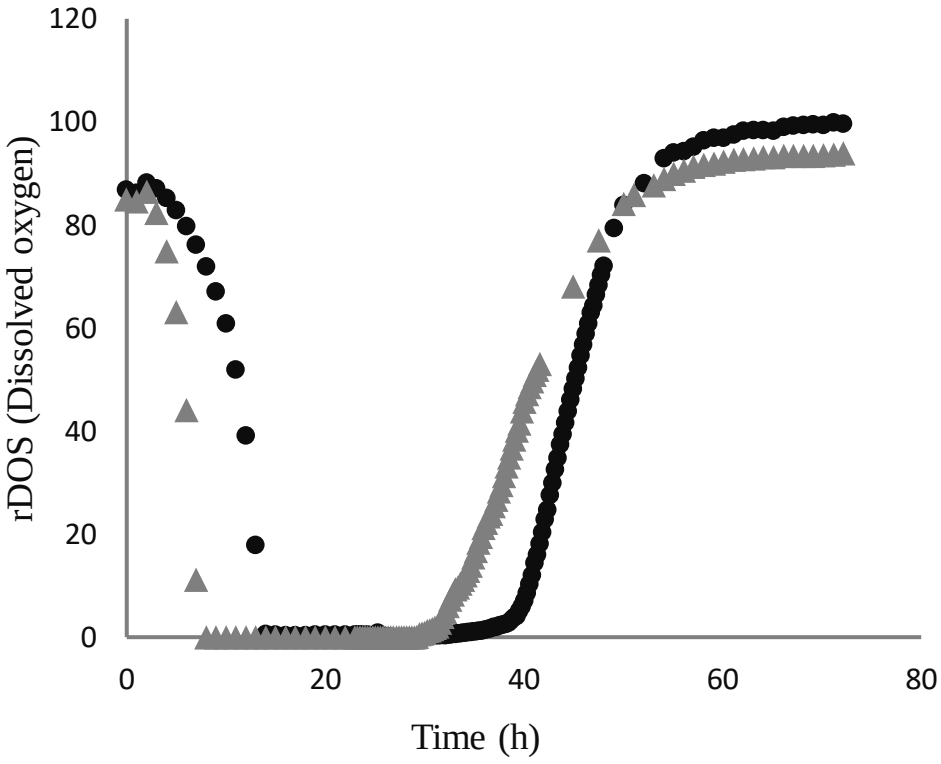

Figure 3.1 AROM3D oxygen measurement in PreSense. Both productions set up with 0.1 mM copper ions and 0.5 mM L-Phe concentration. The dots: Copper ions added initially, the triangle: Copper ions added after 24 hours.

3.3. The model-based optimization for Kriging and Quadratic model

3.3.1. Experimental results of central composite design

In this approach, 24 experiments designed by central composite design were conducted and melanin production was determined from the 24th to the 72nd hour. The data of the selected parameters and melanin titers are given in Table 3.11.

Table 3.11 Titers obtained from points selected by central composite design.

Time of copper addition (hour)	Cu (mM)	L-Phe (mM)	Melanin titer		
			24 h	48 h	72 h
0	**0.23**	**0.30**	0.18	0.52	0.74
5	**0.12**	**0.42**	0.21	0.29	0.30
5	**0.33**	**0.18**	0.12	0.15	0.27
5	**0.33**	**0.42**	0.36	0.44	0.55
5	**0.23**	**0.30**	0.14	0.18	0.30
12	**0.05**	**0.30**	0.09	0.12	0.21
12	**0.40**	**0.30**	0.11	0.18	0.24
12	**0.23**	**0.30**	0.10	0.18	0.24
12	**0.23**	**0.30**	0.12	0.17	0.26
12	**0.23**	**0.30**	0.11	0.17	0.26
12	**0.23**	**0.30**	0.12	0.17	0.30
12	**0.23**	**0.30**	0.12	0.15	0.30
12	**0.23**	**0.30**	0.16	0.18	0.26
12	**0.23**	**0.30**	0.10	0.16	0.27
12	**0.23**	**0.30**	0.14	0.30	0.49
12	**0.40**	**0.30**	0.09	0.19	0.23
12	**0.23**	**0.30**	0.12	0.15	0.24
12	**0.12**	**0.18**	0.11	0.17	0.24
12	**0.23**	**0.30**	0.10	0.15	0.24
19	**0.12**	**0.18**	0.07	0.14	0.15
19	**0.12**	**0.42**	0.07	0.15	0.25
19	**0.33**	**0.18**	0.08	0.17	0.25
19	**0.33**	**0.42**	0.08	0.17	0.29
24	**0.23**	**0.30**	0.04	0.26	0.22

In initial experiments, 48 hours had been identified as the optimal time for melanin production. The results demonstrate that higher L-Phe concentrations yielded better production outcomes compared to lower concentrations. Moreover, the productions

remained consistent across repetitive experiments. When the L-Phe concentration and the timing of copper addition were held constant, but different copper concentrations were employed, the production with higher copper concentrations consistently yielded greater melanin production.

Adding copper after 19 hours did not efficiently produce melanin, and increasing the copper concentration did not lead to improved melanin production. In contrast, the production that added copper ions after 0.5 hours, with very low copper ions and higher L-Phe concentrations, produced more melanin than others. This suggests that adding copper ions earlier resulted in better melanin production. Upon examining the production with 0.12 mM copper added at the 19th hour, it was observed that despite having the same copper and L-Phe concentrations, melanin production remained constant, indicating that increasing the L-Phe concentration did not enhance production. Similarly, looking at the production with 0.33 mM copper added at the 19.6th hour, there was no increase in melanin production even with an increase in L-Phe concentration. Adding copper at the 19th hour did not prove to be efficient. Additionally, when only the copper addition time differed, melanin production increased with earlier copper addition. The best production was achieved with copper added at the beginning. All these results were considered with a focus on the 48th hour, as it was chosen as the optimum production time. No significant changes were observed at the 72nd hour, rendering it inefficient and time-consuming. In the Surwase (2012), tryptone 1.440 g/L , L-Tyr 1.872 g/L and $CuSO_4$ 0.0366 g/L mM were used for melanin production. The actual yield calculated was 1.227 g/L. However, in this thesis tryptone and tyrosine were not used, also, although, copper concentration was 0.0775 g/L, melanin was more produced than Surwase 2012 without L-tyr and tryptone (Surwase., 2012).

3.3.2. Experimental results of random sampling

For randomly selected 12 points, experiments were conducted in triplicate. Melanin titers were determined for various time the 24th to the 72nd hour as given in Table 3.12.

Table 3.12 Titers obtained from randomly selected points.

Time of copper addition (hour)	Cu (mM)	L-Phe (mM)	24	48	72
0.5	**0.07**	**0.20**	0.20	0.30	0.35
0.5	**0.07**	**0.20**	0.23	0.39	0.41
0.5	**0.07**	**0.20**	0.31	0.42	0.46
3.3	**0.18**	**0.12**	0.25	0.35	0.37
3.3	**0.18**	**0.12**	0.28	0.39	0.38
3.3	**0.18**	**0.12**	0.31	0.55	0.48
5.7	**0.22**	**0.28**	0.40	0.63	0.49
5.7	**0.22**	**0.28**	0.27	0.44	0.46
5.7	**0.22**	**0.28**	0.39	0.42	0.43
6.3	**0.33**	**0.36**	0.37	0.47	0.51
6.3	**0.33**	**0.36**	0.36	0.42	0.54
6.3	**0.33**	**0.36**	0.40	0.61	0.63
9.1	**0.12**	**0.15**	0.11	0.22	0.24
9.1	**0.12**	**0.15**	0.09	0.25	0.23
9.1	**0.12**	**0.15**	0.1	0.25	0.24
10.6	**0.36**	**0.45**	0.08	0.26	0.28
10.6	**0.36**	**0.45**	0.12	0.26	0.29
10.6	**0.36**	**0.45**	0.11	0.26	0.34
13.3	**0.14**	**0.40**	0.11	0.19	0.26
13.3	**0.14**	**0.40**	0.10	0.18	0.26
13.3	**0.14**	**0.40**	0.11	0.19	0.25
14.2	**0.29**	**0.33**	0.08	0.11	0.19
14.2	**0.29**	**0.33**	0.08	0.11	0.18
14.2	**0.29**	**0.33**	0.07	0.10	0.19
16.3	**0.1**	**0.5**	0.12	0.20	0.27
16.3	**0.1**	**0.5**	0.11	0.20	0.27
16.3	**0.1**	**0.5**	0.10	0.21	0.26
19.6	**0.24**	**0.24**	0.08	0.15	0.22
19.6	**0.24**	**0.24**	0.08	0.14	0.21
19.6	**0.24**	**0.24**	0.07	0.14	0.21
20.5	**0.39**	**0.21**	0.11	0.19	0.26
20.5	**0.39**	**0.21**	0.11	0.18	0.26
20.5	**0.39**	**0.21**	0.10	0.17	0.25
23.9	**0.28**	**0.38**	0.24	0.20	0.27
23.9	**0.28**	**0.38**	0.03	0.21	0.28
23.9	**0.28**	**0.38**	0.24	0.21	0.27

Experiments conducted under nearly identical production conditions resulted in similar melanin yields. The lowest melanin production was observed when copper was added at 3.3

hours, with concentrations of 0.18 mM for copper and 0.12 mM for L-Phe at the 48th hour. Conversely, the highest melanin production occurred when copper was added after 23.9 hours, with concentrations of 0.28 mM for copper and 0.38 mM for L-Phe at the 48th hour. Contamination was suspected in these productions because achieving melanin production after 24 hours without copper ions is unlikely. In experiments where copper was added simultaneously and in the same quantity, varying L-Phe concentrations did not significantly influence production. Interestingly, even with reduced amounts of copper and L-Phe, production did not decrease when copper was added earlier. For example, the production with 0.33 mM copper added after 6.3 hours, initially with 0.36 mM L-Phe, resulted in 0.61 g/L melanin. In comparison, when 0.18 mM copper was added after 3.3 hours, initially with 0.12 mM L-Phe, it produced 0.55 g/L, indicating minimal difference. This suggests that the timing of copper addition significantly impacts production. The lowest production occurred when copper was added after 23.9 hours, as expected since copper plays a crucial role as a cofactor in the initial 24 hours. High production was achieved with 0.22 mM copper added after 5.7 hours, initially with 0.22 mM L-Phe. However, this production was not substantially different from the one in which 0.18 mM copper was added after 3.3 hours, initially with 0.12 mM L-Phe. This implies that adding copper earlier than 5.7 hours would be more logical.

3.3.3. Model based optimization for melanin production

For model-based optimization, all the experimental data points were used to find the optimum conditions. For this, the two models predicted the best values for the 3 parameters selected for 24, 48, and 72 hours. Then these data points were used to find the optimum conditions that yielded the highest melanin titers in table 3.13.

Table 3.13 Actual melanin titers under optimal conditions (initially added copper ion and 0.5 mM L-Phe).

	Melanin titer (g/L)		
	Cu (mM)		
Time	**0.27**	**0.31**	**0.4**
24	0.23	0.17	0.13
48	0.83	0.91	0.63
72	0.96	1.03	0.77

For both the Kriging and Quadratic models, initial copper addition was the optimal time. Additionally, when copper was added initially, the optimal L-Phe concentration was at 0.5 mM. Under the conditions of a copper concentration of 0.4 mM, the titers for the Quadratic model remained consistent at 24, 48, and 72 hours. However, for the Kriging model, the titers varied at 24, 48, and 72 hours for different copper concentrations of 0.27, 0.31, and 0.4 mM. The expected melanin titer was determined to be 0.75 g/L based on the initial melanin production experiments with Cg-EKV-I. The lowest melanin titer was found with 0.4 mM copper ion. There was no high difference between 0.31 mM and 0.27 mM copper concentrations. The best melanin production was calculated at 0.91 g/L with 0.27 mM copper concentration. Both the Kriging and Quadratic models demonstrated successful representation of the dataset from which they were created, as indicated by their respective values. Based on the OD_{600} data, growth was observed from 24 to 72 hours. Experiments with the same copper and L-Phe concentrations but varying copper addition times exhibited almost identical growth rates, indicating that copper addition time had minimal impact. As expected, a decrease in L-Phe concentrations corresponded to a reduction in growth. Additionally, earlier copper addition led to decreased growth, as copper hindered AROM3D growth. The lowest growth was observed when copper was added at the beginning of production. Repeated experiments consistently showed almost the same results. The results indicate that, in two productions with the same amount of copper added at the same time but different L-Phe concentrations, higher L-Phe concentration led to greater growth, emphasizing the effect of L-Phe on growth. Likewise, a decrease in L-Phe concentration coupled with an increase in copper concentration resulted in decreased growth.

3.4. Purification of melanin

After the optimization of the melanin, it was purified as described in Section 2.3. Two different production conditions were used, as shown in Table 3.14. These productions were carried out in two separate flasks with volumes of 25 mL and 50 mL respectively and stirring speeds of 150 and 180 rpm were examined to observe variations in melanin production. When considering volume, it was observed that 50 mL volumes resulted in higher yields compared to 25 mL. Productions using 25 mL volumes did not yield similar results and were considered unsuitable for purification. On the other hand, 50 mL volume productions provided calculations with similar yields, making it the most suitable volume for purification purposes. In terms of stirring speed, there was no significant difference between 150 and 180 rpm. The optimum value was determined to be 150 rpm due to energy consumption considerations. However, the yield was not efficient for melanin purification. In Guo (2014), yeast was used extensively, which may complicate the purification process. In addition, the use of Amylodextrine may also hinder purification. Therefore, it is advisable to use more simple media. Consequently, yeast and its derivatives were not used in our study (Guo., 2014).In the Kraseasintra (2023) Yeast extract, soluble starch and HAO-DBRH were used. The inclusion of yeast, starch and HAO-DBRH in the study makes the purification process much more challenging (Kraseasintra., 2023). According to the Surwase (2012), tryptone was employed, making the purification process more challenging (Surwase., 2012). The use of tryptone probably made the medium more complex and economically more expensive than ours. Our medium is simpler in composition. Therefore, our purification process should be simpler and cost-effective.

Table 3.14 The yields result from the purification of melanin with different growth conditions.

Volume (mL)	**Yield (mg Mel / mg L-Tyr) 150 rpm**	**Yield (mg Mel / mg L-Tyr) 180 rpm**
50	0.2±0.03	0.2±0.02
25	0.5±0.4	0.3±0.2

3.5. Melanin analysis

3.5.1. HPLC analysis of melanin

Figure 3.2 shows an analysis of melanin with an HPLC at 50 °C. When examining the experiments conducted at 25 and 70 degrees, it was observed that the peaks were not sufficiently separated, which prevented us from making a detailed analysis. When experiments conducted at 35 degrees were examined, it was noticed that two peaks were not sufficiently separated, indicating that the temperature was not suitable. At 50 degrees, the peaks were most clearly separated, making it the optimal temperature. The peak corresponding to the melanin pigment is clearly visible, facilitating accurate and easy analysis. Therefore, the optimum temperature was selected as 50°C.

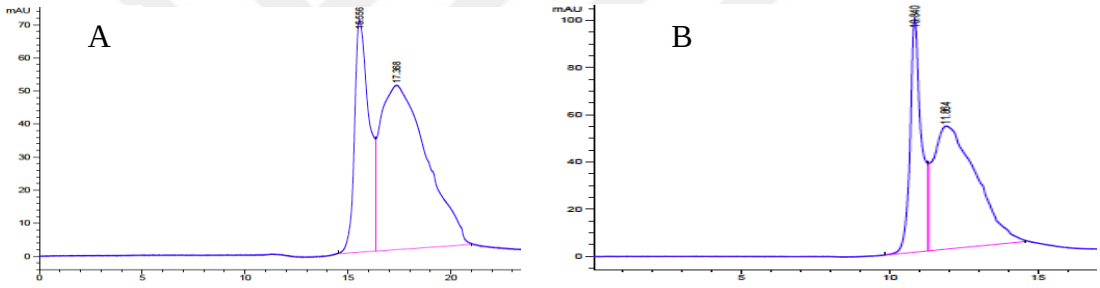

Figure 3.2 A) 1 g/L Standard melanin analysis B) 1 g/L purified melanin with HPLC at 50 °C

3.5.2. UV-Vis analysis of melanin

According to the Figure 3.3, the absorbance decreased continuously as the wavelength increased from 200 to 800 nm. There was a linear correlation between wavelength and log absorbance which is an important issue for the characterization of melanin. This can be related to the percentage of absorption is greatest in the UV region (Raman & Ramasamy, 2017).

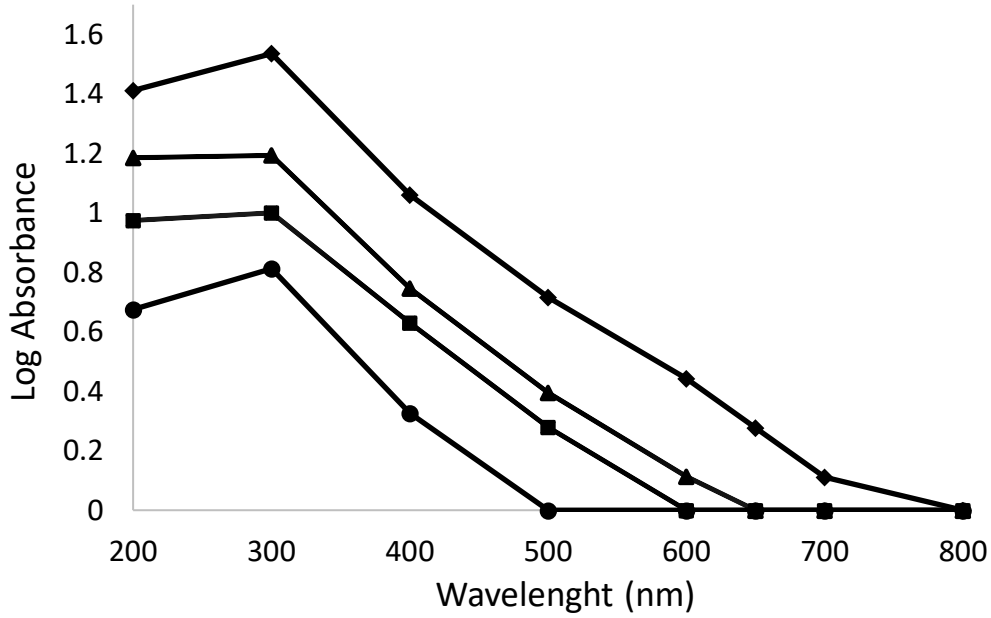

Figure 3.3 Relationship between log absorbance and wavelength from 200 to 800 nm on purified melanin. The lines show 0.25 g/L, the triangles show 0.125 g/L, the squares show 0.1 g/L, and the dots show 0.05 g/L of purified melanin.

3.5.3. FT/IR analysis of melanin

A broad absorption band centered around 3422 cm^{-1} was observed, as depicted in Figure 3.4. This large absorption band is indicative of the O-H or N-H stretching vibration modes. The presence of carboxylic acid, phenolic, and aromatic amino functions in the indolic and pyrrolic systems is suggested to contribute to this broad absorption between 3600 and 3200 cm^{-1} spectral regions. Specifically, the peak associated with this band was identified at 3438 cm^{-1}. Other observed peaks include those at 2917, 2839, 1621, 1464, 1374, 1038, and 661, as reported by Mbonyiryivuze et al. (2015). In work described by Kiran 2017 ccharacteristics peaks were observed at 3264 cm^{-1}, 2924.56 cm^{-1}, 1622.84 cm^{-1}, 1529.27 cm^{-1}, 1412.64 cm^{-1}, 1216.86 cm^{-1}, 1041.37 cm^{-1}, 611 cm^{-1}, as seen in Figure 9. Those peaks are quite similar to peak obtained by FTIR analysis for melanin produced in this work.

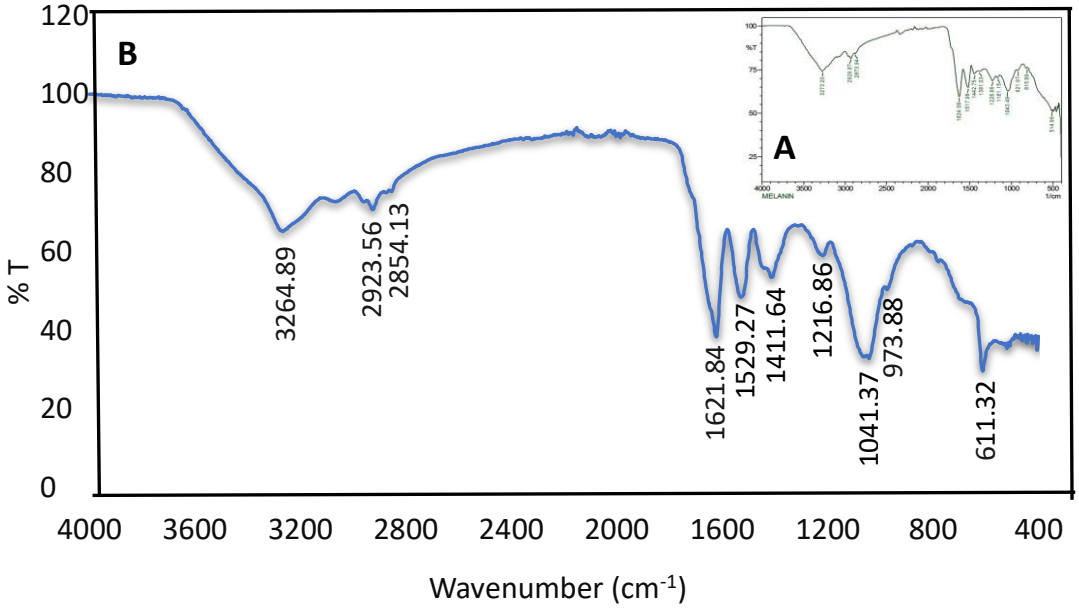

Figure 3.4 A) FTIR analysis of melanin (Kiran., 2017) B) Analysis of purified melanin

Two absorption peaks associated with the stretching vibration of the aliphatic C-H group were observed: a weak peak at 2839 cm^{-1} and a medium-intensity band at 2917 cm^{-1}. These frequencies align well with those reported in the literature. The presence of distinct surroundings for hydrogen atoms in various components of sepia may explain the observation of two slightly different frequencies for CH stretching. Apart from the C=O double bond (COOH) of the carboxylic function, the bending vibration modes of the aromatic ring C=C and C=N bonds in the aromatic system contribute to a prominent, strong band at 1621 cm (within the range of 1647 - 1531 cm^{-1}). Weak bands below 700 cm^{-1} in the melanin pigment are attributed to alkene C-H substitution, while the mode between 1468 and 1330 cm^{-1} may result from aliphatic C-H groups (Kiran et al., 2017). The OH bending of the carboxylic and phenolic groups, indicating the Indole ring vibration/CNC stretching, is manifested in the 1400–1300 cm^{-1} region, specifically at the peak centered at 1374 cm^{-1}. The in-plane/out-of-plane deformation of the CH is represented by the peak with a center of 1038 cm^{-1}. Ultimately, the weak bands below 700 cm^{-1} in sepia melanin are attributed to the out-of-plane bending of the aromatic carbon-hydrogen bond (Tarangini 2014).

3.5.4. SEM analysis of melanin

To validate the melanin production in this study, the Scanning Electron Microscope (SEM) technique was utilized, and the outcomes are depicted in Figure 3.5. The SEM analysis provided insights into the morphological characteristics and structural arrangement of the pigment extracted from *C. glutamicum*. The results revealed that the pigment exhibits a unique crystal shape, reminiscent of structures seen in yeast cells (Elsayis., 2022). The average size of the extracted pigment particles was determined to be around 1.83 µm ±0.35.

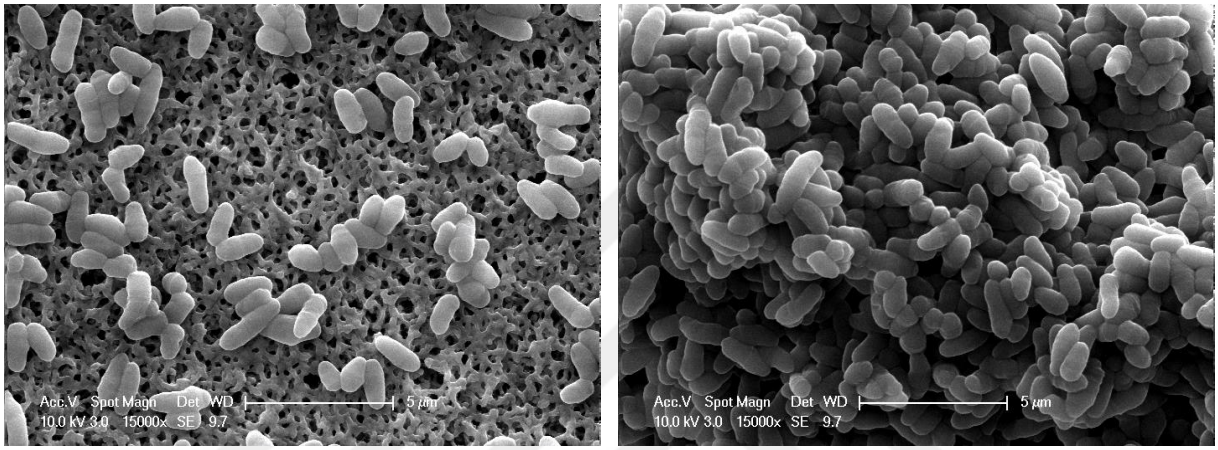

Figure 3.5 Images obtained from SEM with purified melanin.
(Magnitude 15000x, size 5µm)

3.6. Melanin production with orange peel hydrolysate with Cg-EKV-II

Melanin was produced with Cg-EKV-II strain grown on orange peel hydrolysate and the results are given in Table 3.15. It was seen that there was no huge melanin production difference between room temperature and 30 °C. So, it can be said that for production room temperature can be used. This could help to save energy. Also, there was no vital melanin production difference between non-shaking and shaking (150 rpm) conditions. According to all these results, melanin can be produced at room temperature and non-shaking. This production way has many advantages such as low cost, ease, and environmental issues. The optimum cell amount was obtained at 1.12 mg cells.

Table 3.15 Whole-cell bio-fermentation melanin production with CgEKV-II after 24 hours with 100 µL copper ions.

Cell amount (mg)	Melanin (mg/L) (room temperature, 0 rpm)	Melanin (mg/L) (30°, 150 rpm)
0.14	4.6	4.6
0.28	6.8	2.8
0.42	4.4	4.2
0.56	7.0	9.1
0.70	6.1	9.6
0.84	10.6	6.3
0.98	6.2	8.1
1.12	11.2	9.2
1.26	9.9	11.2

4. CONCLUSION

Pigments are colored materials that hold significant economic value globally, estimated to be worth around 30 billion dollars in the industry. It is crucial to reduce the production cost of melanin. This study aims to optimize the production of melanin, a biological pigment and agricultural waste, to attain optimal conditions for the cultivation of commercially significant bacteria, *C. glutamicum*. Melanin was produced using three different strains. In these experiments, CGXII minimal medium was utilized as a carbon source for the cultivation of AROM3 harboring pEKEx3-tyr_{Rs}, *C. glutamicum* ATCC 13032 harboring pEKEx2-tyr_{Rs}, and EKV-I harboring pEKEx3-$xylA_{Xc}$-$xylB_{Cg}$. Firstly, melanin production conditions were selected with CgEKV-I. Among various production methods, AROM3D was chosen for optimization due to its lack of requirement for L-tyr, making it a cost-effective and environmentally friendly method. Before optimization, 0.75 g/L melanin was produced with 1 g/L L-Tyr and 0.1 mM Cu after 48 hours. Then, production without L-Tyr addition in AROM3D cells was achieved. Experiments with three independent variables for melanin production were designed using a statistical approach, and then Quadratic and Kriging models were used to find the optimal production conditions. Three self-sustaining variables for melanin production were copper concentration, copper addition time, and L-Phe concentration. After optimization, an optimum copper concentration of 0.31 mM, L-Phe concentration of 0.5 mM, and initial copper addition time were obtained under the optimum conditions, and melanin titer was 1.03 g/L after 72 hours under these conditions. The resulting melanin underwent quality control through HPLC, SEM, UV/Vis, and FT/IR analyses, all of which yielded excellent results. Subsequently, the obtained melanin was purified using various methods. Although the purification results were not highly efficient, the absence of additional substrates made purification easier. Lastly, melanin was produced using orange peel hydrolysate, a method that was cost-effective, simple, and environmentally friendly. Cell amount, rpm, and temperature were optimized using this technique. The primary advantages of whole-cell biocatalysis include the use of inexpensive (orange peel hydrolysate) and abundant raw materials, as well as the ability to catalyze multistep reactions. In the future, this whole-cell biocatalysis method can be further developed and refined for melanin production using food waste. According to table 1.2, melanin production from different sources was analyzed. The purification of productions containing yeast, starch, casein, peptone, and tryptone is very difficult; therefore, none of these products were used in this study. Melanin production took only 2 days, which is a

shorter duration compared to most studies. According to the table, using bacteria instead of fungi not only shortened the duration of the study but also made the working conditions easier. Additionally, *C. glutamicum* compared to other bacteria has many advantages: it is engineered to secrete amino acids, is a safe strain for humans (GRAS), displays rapid growth to high cell densities, has genetic stability due to the lack of a recombination repair system, and has an extensive spectrum of carbon usage. Furthermore, since waste was used as a substrate, an economic advantage was achieved compared to other studies. Although tyrosine is used in most studies, melanin production was achieved without the use of tyrosine in this study. Unlike other studies, production was carried out without the need for an additional metal ion. Considering all this, this work was achieved in the cheapest, fastest, and most environmentally friendly way

REFERENCES

Ahn, S. Y., Jang, S., Sudheer, P. D. V. N., & Choi, K. Y. (2021). Microbial Production of Melanin Pigments from Caffeic Acid and L-Tyrosine Using Streptomyces glaucescens and FCS-ECH-Expressing Escherichia coli. *International Journal of Molecular Sciences*, *22*(5), 1–15. https://doi.org/10.3390/IJMS22052413

Almeida-Paes, R., Nosanchuk, J. D., & Zancope-Oliveira, R. M. (2012). *Fungal melanins: Biosynthesis and biological functions* (pp. 77–107). Nova Science Publishers, Inc. https://einstein.pure.elsevier.com/en/publications/fungal-melanins-biosynthesis-and-biological-functions-2

Amooghin, A. E., Pedram, M. Z., Omidkhah, M., & Yegani, R. (2013). A novel CO2-selective synthesized amine-impregnated cross-linked polyvinylalcohol/glutaraldehyde membrane: fabrication, characterization, and gas permeation study. *Greenhouse Gases: Science and Technology*, *3*(5), 378–391. https://doi.org/10.1002/GHG.1369

Araujo, M., Xavier, J. R., Nunes, C. D., Vaz, P. D., & Humanes, M. (2012). Marine sponge melanin: A new source of an old biopolymer. *Structural Chemistry*, *23*(1), 115–122. https://doi.org/10.1007/S11224-011-9843-7/FIGURES/3

Ayala, J. R., Montero, G., Coronado, M. A., García, C., Curiel-Alvarez, M. A., León, J. A., Sagaste, C. A., & Montes, D. G. (2021). Characterization of Orange Peel Waste and Valorization to Obtain Reducing Sugars. *Molecules 2021, Vol. 26, Page 1348*, *26*(5), 1348. https://doi.org/10.3390/MOLECULES26051348

Bayram, S.; Dengiz, C.; Gerçek, Y.C.; Cetin, I.; Topcul, M.R. (2020) Bioproduction, structure elucidation, and in vitro antiproliferative effect of eumelaninpigmentfrom *Streptomyces* parvus BSB49. *Arch. Microbiol.*, *202*, 2401–2409.

Beltrán-García, M. J., Prado, F. M., Oliveira, M. S., Ortiz-Mendoza, D., Scalfo, A. C., Pessoa, A., Medeiros, M. H. G., White, J. F., & Di Mascio, P. (2014). Singlet Molecular Oxygen Generation by Light-Activated DHN-Melanin of the Fungal Pathogen Mycosphaerella fijiensis in Black Sigatoka Disease of Bananas. *PLOS ONE*, *9*(3), e91616. https://doi.org/10.1371/JOURNAL.PONE.0091616

Borovanskỳ, J., & Riley, P. A. (2011). Physiological and Pathological Functions of Melanosomes. *Melanins and Melanosomes: Biosynthesis, Biogenesis, Physiological,*

and Pathological Functions, 343–381. https://doi.org/10.1002/9783527636150.CH12

Büngeler, A., Hämisch, B., Huber, K., Bremser, W., & Strube, O. I. (2017). Insight into the Final Step of the Supramolecular Buildup of Eumelanin. *Langmuir*, *33*(27), 6895–6901. https://doi.org/10.1021/ACS.LANGMUIR.7B01634/ASSET/IMAGES/MEDIUM/LA-2017-01634U_0006.GIF

Cao, W., Zhou, X., McCallum, N. C., Hu, Z., Ni, Q. Z., Kapoor, U., Heil, C. M., Cay, K. S., Zand, T., Mantanona, A. J., Jayaraman, A., Dhinojwala, A., Deheyn, D. D., Shawkey, M. D., Burkart, M. D., Rinehart, J. D., & Gianneschi, N. C. (2021). Unraveling the structure and function of melanin through synthesis. *Journal of the American Chemical Society*, *143*(7),2622–2637. https://doi.org/10.1021/JACS.0C12322/ASSET/IMAGES/MEDIUM/JA0C12322_0012.GIF

Carus, M., Dammer, L., Raschka, A., & Skoczinski, P. (2020). Renewable carbon: Key to a sustainable and future-oriented chemical and plastic industry: Definition, strategy, measures and potential. *Greenhouse Gases: Science and Technology*, *10*(3), 488–505. https://doi.org/10.1002/GHG.1992

Centeno, S. A., & Shamir, J. (2008). Surface enhanced Raman scattering (SERS) and FTIR characterization of the sepia melanin pigment used in works of art. *Journal of Molecular Structure*, *873*(1–3), 149–159. https://doi.org/10.1016/J.MOLSTRUC.2007.03.026

Choi, K.Y., (2021). Bioprocess of Microbial Melanin Production and Isolation. Front Bioeng Biotechnol.doi: 10.3389/fbioe.2021.765110. eCollection 2021.

Cordero, R. J. B., & Casadevall, A. (2017). Functions of fungal melanin beyond virulence. *Fungal Biology Reviews*, *31*(2), 99–112. https://doi.org/10.1016/J.FBR.2016.12.003

Costa, T. G., Younger, R., Poe, C., Farmer, P. J., & Szpoganicz, B. (2012). Studies on synthetic and natural melanin and its affinity for Fe(III) ion. *Bioinorganic Chemistry and Applications, 2012*. https://doi.org/10.1155/2012/712840

Coyne, V. E., & Al-Harthi, L. (1992). Induction of melanin biosynthesis in Vibrio cholerae. *Applied and Environmental Microbiology*, *58*(9), 2861–2865. https://doi.org/10.1128/AEM.58.9.2861-2865.1992

d'Ischia, M., Wakamatsu, K., Cicoira, F., Di Mauro, E., Garcia-Borron, J. C., Commo, S., Galván, I., Ghanem, G., Kenzo, K., Meredith, P., Pezzella, A., Santato, C., Sarna, T.,

Simon, J. D., Zecca, L., Zucca, F. A., Napolitano, A., & Ito, S. (2015). Melanins and melanogenesis: from pigment cells to human health and technological applications. *Pigment Cell & Melanoma Research*, *28*(5), 520–544. https://doi.org/10.1111/PCMR.12393

D'Ischia, M., Wakamatsu, K., Napolitano, A., Briganti, S., Garcia-Borron, J. C., Kovacs, D., Meredith, P., Pezzella, A., Picardo, M., Sarna, T., Simon, J. D., & Ito, S. (2013). Melanins and melanogenesis: Methods, standards, protocols. *Pigment Cell and Melanoma Research*, *26*(5), 616–633. https://doi.org/10.1111/PCMR.12121

Eggeling, L., & Sahm, H. (1999). L-glutamate and L-lysine: Traditional products with impetuous developments. *Applied Microbiology and Biotechnology*, *52*(2), 146–153. https://doi.org/10.1007/S002530051501/METRICS

Eisenman, H. C., & Casadevall, A. (2012). Synthesis and assembly of fungal melanin. *Applied Microbiology and Biotechnology*, *93*(3), 931–940. https://doi.org/10.1007/S00253-011-3777-2

El- Naggar, N., E.-A., & E.-E., & S. M. (2017). Bioproduction, characterization, anticancer and antioxidant activities of extracellular melanin pigment produced by newly isolated microbial cell factories *Streptomyces glaucescens NEAE-H*. Scientific Reports, 7(1) https://doi.org/10.1038/srep42129

El-Naggar, N.; Saber, W. (2022) Natural melanin: Current trends, and future approaches, with especial reference to microbial source. *Polymers*, *14*, 1339

Elsayis A., Sahar W. M. Hassan, Khaled M. Ghanem and Heba Khairy, (2022) Optimization of melanin pigment production from the halotolerant black yeast Hortaea werneckii AS1 isolated from solar salter in Alexandria, Department of Botany and Microbiology, Faculty of Science, Alexandria University, Alexandria, Egypt

El-Zawawy, N.A.; Kenawy, E.-R.; Ahmed, S.; El-Sapagh, S. (2024), Bioproduction and optimization of newly characterized melanin pigment from *Streptomycesdjakartensis* NSS-3 with its anticancer, antimicrobial,and radioprotective properties. *Microb.Cell Fact. 23*, 23

Eskandari, S., & Etemadifar, Z. (2021). Melanin biopolymers from newly isolated Pseudomonas koreensis strain UIS 19 with potential for cosmetics application, and optimization on molasses waste medium. *Journal of Applied Microbiology*, *131*(3), 1331–1343. https://doi.org/10.1111/JAM.15046

Farmer, W. R., & Liao, J. C. (2000). Improving lycopene production in Escherichia coli by engineering metabolic control. *Nature Biotechnology*, *18*(5), 533–537. https://doi.org/10.1038/75398

Fogarty, R. V. & T. J. M. (1996). Fungal melanins and their interactions with metals. Enzyme and Microbial Technology, 19(4), 311–317 | 10.1016/0141-0229(96)00002-6. https://doi.org/10.1016/0141-0229(96)00002-6

Ganesh Kumar, C., Sahu, N., Narender Reddy, G., Prasad, R. B. N., Nagesh, N., and Kamal, A. (2013). Production of Melanin Pigment from Pseudomonas Stutzeri Isolated from Red Seaweed Hypnea Musciformis. *Lett. Appl. Microbiol.* 57, 295–302. doi:10.1111/lam.12111

Ghadge, V., Kumar, P., Singh, S., Mathew, D. E., Bhattacharya, S., Nimse, S. B., et al. (2020). Natural Melanin Produced by the Endophytic Bacillus Subtilis 4NP-BL Associated with the Halophyte Salicornia Brachiata. *J. Agric. Food Chem.* 68, 6854–6863. doi:10.1021/acs.jafc.0c01997

Ghadge, V.; Kumar, P.; Maity, T.K.; Prasad, K.; Shinde, P.B. (2022), Facile alternative sustainable process for the selective extraction of microbial melanin. *ACS Sustain. Chem. Eng. 10*, 2681–2688

Gibson, L. F., & George, A. M. (1998). Melanin and novel melanin precursors from Aeromonas media. *FEMS Microbiology Letters*, *169*(2), 261–268. https://doi.org/10.1111/J.1574-6968.1998.TB13327.X

Gokgoz B., N., Avci, F. G., Yoneten, K. K., Alaybeyoglu, B., Ozkirimli, E., Sayar, N. A., B. Sariyar Akbulut, B. (2017). Response of Escherichia coli to Prolonged Berberine Exposure. Microbial Drug Resistance, 23(5), 531–544. doi:10.1089/mdr.2016.0063

Gowri, P. M. & S. S. (1996). *Encapsulation as a response of Azospirillum brasilense sp7 to zinc stress. World Journal of Microbiology & Biotechnology, 12(4), 319–322 | 10.1007/bf00340207*. https://doi.org/10.1007/BF00340207

Guo, J., Rao, Z., Yang, T., Man, Z., Xu, M., & Zhang, X. (2014). High-level production of melanin by a novel isolate of *Streptomyces kathirae*. FEMS Microbiology Letters, 357(1), 85–91. doi:10.1111/1574-6968.12497

Hagiwara, K. , Okura, M. , Kuno, A. , Horio, Y. , & & Yamashita, T. (2016). Biochemical effects of the flavanol-rich lychee fruit extract on the melanin biosynthesis and reactive oxygen species. The Journal of Dermatology, 43(10), 1174–1183 The Journal of Dermatology. https://doi.org/10.1111/1346-8138.13326

Hamano, P. S. , & Kilikian, B. V. (2006, December). Production of red pigments by *Monascus ruber* in culture media containing corn steep liquor. Brazilian Journal of Chemical Engineering, 23(4), 443–449 Brazilian Journal of Chemical Engineering. https://doi.org/10.1590/S0104-66322006000400002

Ikeda, M. (2003). Amino acid production processes. Advances in Biochemical Engineering/Biotechnology, *79*, 1–35. https://doi.org/10.1007/3-540-45989-8_1

Inamdar, S., Joshi, S., Bapat, V., & Jadhav, J. (2014). Innovative use of Mucuna monosperma (Wight) callus cultures for continuous production of melanin by using statistically optimized biotransformation medium. *Journal of Biotechnology*, *170*(1), 28–34. https://doi.org/10.1016/J.JBIOTEC.2013.11.012

Jalmi P, Bodke P, Wahidullah S, Raghukumar S (2012) The fungus Gliocephalotrichum simplex as a source of abundant, extracellular melanin for biotechnological applications. World J Microbiol Biotechnol 28:505–512. https://doi.org/10.1007/s11274-011-0841-0

Kazi, Z.; Hungund, B.S.; Yaradoddi, J.S.; Banapurmath, R.; Yusuf, A.A.; Kishore, K.L.; Soudagar, M.E.M.;Khan,T.M.Y.;Elfasakhany,A.;Buyondo,K.A.(2022), Production,Characterization,andAntimicrobial Activity of Pigment from *Streptomyces* Species. *J. Biomater. Appl. 2022*, 3962301

Keilhauer C. , L. Eggeling, H. Sahm. (1993). Isoleucine synthesis in Corynebacterium glutamicum: molecular analysis of the ilvB-ilvN-ilvC operon. JOURNAL OF BACTERIOLOGY, p. 5595-5603

Kimura, A., Adachi, N., & Horikoshi, M. (2003). Series of vectors to evaluate the position and the order of two different affinity tags for purification of protein complexes. *Analytical Biochemistry*, *314*(2), 253–259. https://doi.org/10.1016/S0003-2697(02)00664-4

Kinoshita, S., Udaka, S., & Shimono, M. (1957). Studies On the Amino Acid Fermentation Part I. Production of L-Glutamic Acid by Various Microorganisms∗. *The Journal of General and Applied Microbiology*, *3*(3), 193–205. https://doi.org/10.2323/JGAM.3.193

Kiran, G. S., Dhasayan, A., Lipton, A. N., Selvin, J., Arasu, M. V., & Al-Dhabi, N. A. (2014). Melanin-templated rapid synthesis of silver nanostructures. *Journal of Nanobiotechnology*, *12*(1). https://doi.org/10.1186/1477-3155-12-18

Kiran, G. S., Jackson, S. A., Priyadharsini, S., Dobson, A. D. W., & Selvin, J. (2017). Synthesis of Nm-PHB (nanomelanin-polyhydroxy butyrate) nanocomposite film and its protective effect against biofilm-forming multi drug resistant *Staphylococcus aureus* . *Scientific Reports, 7(1)*. doi:10.1038/s41598-017-08816-y

Kleijnen, J. P. C. (2017). *Kriging: Methods and Applications. SSRN Electronic Journal*. doi:10.2139/ssrn.3075151 Tilburg University, Postbox 90153, 5000 LE Tilburg, Netherlands

Kraseasintra, O.; Sensupa,S.; Mahanil, K.; Yoosathaporn, S.;Pekkoh, J.; Srinuanpan, S.;Pathom-aree, W.; Pumas, C. (2023). Optimization of Melanin Production by *Streptomyces antibioticus NRRLB-1701 Using* Arthrospira (Spirulina) platensis Residues Hydrolysates as Low-Cost L-tyrosine Supplement.BioTech,12, 24

Kumar, R. R. , & P. S. (2011). Metabolic Engineering of Bacteria. Indian Journal of Microbiology, 51(3), 403–409

Kurpejović, E., Burgardt, A., Bastem, G. M., Junker, N., Wendisch, V. F., & Sariyar Akbulut, B. (2023). Metabolic engineering of Corynebacterium glutamicum for l-tyrosine production from glucose and xylose. *Journal of Biotechnology*, *363*, 8–16. https://doi.org/10.1016/J.JBIOTEC.2022.12.005

Kurpejović, E., Wendisch, V. F., & Sariyar Akbulut, B. (2021). Tyrosinase-based production of L-DOPA by Corynebacterium glutamicum. *Applied Microbiology and Biotechnology*, *105*(24), 9103–9111. https://doi.org/10.1007/S00253-021-11681-5

Lagunas-Munoz, V. H. C.-V. N. , B. F. , G. G. , & M. A. J. of A. M. (2006). Optimum melanin production using recombinant *Escherichia coli*. Journal of Applied Microbiology, 101(5), 1002–1008

Lee, F. C., Pandu Rangaiah, G., & Lee, D. Y. (2010). Modeling and optimization of a multi-product biosynthesis factory for multiple objectives. *Metabolic Engineering*, *12*(3), 251–267. https://doi.org/10.1016/J.YMBEN.2009.12.003

Lee, J. Y., Na, Y. A., Kim, E., Lee, H. S., & Kim, P. (2016). The Actinobacterium Corynebacterium glutamicum, an Industrial Workhorse. *Journal of Microbiology and Biotechnology*, *26*(5), 807–822. https://doi.org/10.4014/JMB.1601.01053

Lee, J., Saddler, J. N., Um, Y., & Woo, H. M. (2016). Adaptive evolution and metabolic engineering of a cellobiose- and xylose- negative Corynebacterium glutamicum that co-utilizes cellobiose and xylose. *Microbial Cell Factories*, *15*(1), 1–16. https://doi.org/10.1186/S12934-016-0420-Z/FIGURES/8

Lefevre, C. E. , & & Perrett, D. I. (2015). Fruit over sunbed: Carotenoid skin colouration is found more attractive than melanin colouration. Quarterly Journal of Experimental Psychology. https://doi.org/10.1080/17470218.2014.944194

Li, C., Ji, C., & Tang, B. (2018). Purification, characterisation and biological activity of melanin from *Streptomyces sp*. *FEMS Microbiology Letters*, *365*(19), 1–8. https://doi.org/10.1093/FEMSLE/FNY077

Liu, D., Wei, L., Guo, T., & Tan, W. (2014). Detection of DOPA-Melanin in the Dimorphic Fungal Pathogen Penicillium marneffei and Its Effect on Macrophage Phagocytosis In Vitro. *PLOS ONE*, *9*(3), e92610. https://doi.org/10.1371/JOURNAL.PONE.0092610

Mahmutoglu, G., Topsakal, A., Altan, E., Kuskonmaz, N., Daglilar, S., Oktar, F. N., Erdemir, G., Kuruca, S. E., Akyol, S., Gunduz, O., & Ben-Nissan, B. (2023). Effects of temperature and pH on the synthesis of nanohydroxyapatite powders by chemical precipitation. *Journal of the Australian Ceramic Society*. https://doi.org/10.1007/s41779-023-00927-2

Manivasagan P, Venkatesan J, Senthilkumar K et al (2013) Isolation and characterization of biologically active melanin from Actinoalloteichus sp. MA-32. Int J Biol Macromol 58:263–274. https://doi.org/10.1016/j.ijbiomac.2013.04.041

Mbonyiryivuze, A., Nuru, Z. Y., Ngom, B. D., Mwakikunga, B., Dhlamini, S. M., Park, E., & Maaza, M. (2015). Morphological and Chemical Composition Characterization of Commercial Sepia Melanin. *American Journal of Nanomaterials, Vol. 3, 2015, Pages 22-27*, *3*(1), 22–27. https://doi.org/10.12691/AJN-3-1-3

Melanin | C18H10N2O4 - PubChem. (n.d.). Retrieved April 26, 2023, from https://pubchem.ncbi.nlm.nih.gov/compound/Melanin#section=2D-Structure

Nakayama, K., Tanaka, H., Hagino, H., & Kinoshita, S. (1966). Studies on Lysine Fermentation:Part V. Concerted Feedback Inhibition of Aspartokinase and the Absence of Lysine Inhibition on Aspartic Semialdehyde-Pyruvate Condensation in Micrococcus glutamicus. *Agricultural and Biological Chemistry*, *30*(6), 611–616. https://doi.org/10.1080/00021369.1966.10858649

Nosanchuk, J. D., & Casadevall, A. (2003). The contribution of melanin to microbial pathogenesis. *Cellular Microbiology*, *5*(4), 203–223. https://doi.org/10.1046/J.1462-5814.2003.00268.X

Novellino, L., Napolitano, A., & Prota, G. (2000). Isolation and characterization of mammalian eumelanins from hair and irides. *Biochimica et Biophysica Acta*, *1475*(3), 295–306. https://doi.org/10.1016/S0304-4165(00)00080-5

Patil, S., Sistla, S., Bapat, V., & Jadhav, J. (2018). Melanin-Mediated Synthesis of Silver Nanoparticles and Their Affinity Towards Tyrosinase 1. *Applied Biochemistry and Microbiology*, *54*(2), 163–172. https://doi.org/10.1134/S0003683818020096

Pavan, M. E., López, N. I., & Pettinari, M. J. (2020). Melanin biosynthesis in bacteria, regulation and production perspectives. *Applied Microbiology and Biotechnology*, *104*(4), 1357–1370. https://doi.org/10.1007/S00253-019-10245-Y

Plonka M. P., & Grabacka M. (2006). *Melanin synthesis in microorganisms--biotechnological and medical aspects - PubMed*. Acta Biochim Pol. https://pubmed.ncbi.nlm.nih.gov/16951740/

Polapally, R.; Mansani, M.; Rajkumar, K.; Burgula, S.; Hameeda, B.; Alhazmi, A.; Bantun, F.; Almalki, A.H.; Haque, S.; El Enshasy, H.A.; et al. (2022) Melanin pigment of Streptomycespuniceus RHPR9 exhibits antibacterial, antioxidant, and anticancer activities. PLoS ONE , 17, e0197709

Prados-Rosales, R., Toriola, S., Nakouzi, A., Chatterjee, S., Stark, R., Gerfen, G., Tumpowsky, P., Dadachova, E., & Casadevall, A. (2015). Structural characterization of melanin pigments from commercial preparations of the edible mushroom Auricularia auricula. *Journal of Agricultural and FoodChemistry*,*63*(33),7326–7332 https://doi.org/10.1021/ACS.JAFC.5B02713/ASSET/IMAGES/MEDIUM/JF-2015027132_0006.GIF

Pralea, I. E., Moldovan, R. C., Petrache, A. M., Ilieș, M., Hegheș, S. C., Ielciu, I., Nicoară, R., Moldovan, M., Ene, M., Radu, M., Uifălean, A., & Iuga, C. A. (2019). From extraction to advanced analytical methods: The challenges of melanin analysis. In *International Journal of Molecular Sciences* (Vol. 20, Issue 16). MDPI AG. https://doi.org/10.3390/ijms20163943

Pralea, I.-E., Moldovan, R.-C., Petrache, A.-M., Ilies, M., Ielciu, I., Nicoară, R., Moldovan, M., Ene, M., Radu, M., Uifălean, A., & Iuga, C.-A. (2019). *Molecular Sciences Review From Extraction to Advanced Analytical Methods: The Challenges of Melanin Analysis*. https://doi.org/10.3390/ijms20163943

Prota, G. (1995). The chemistry of melanins and melanogenesis. *Fortschritte Der Chemie Organischer Naturstoffe = Progress in the Chemistry of Organic Natural Products.*

Progres Dans La Chimie Des Substances Organiques Naturelles, *64*, 93–148. https://doi.org/10.1007/978-3-7091-9337-2_2

Qi, Y. , Liu, J. , Liu, Y. , Yan, D. , Wu, H. , Li, R. , & Ren, X. (2020). Polyphenol oxidase plays a critical role in melanin formation in the fruit skin of persimmon (Diospyros kaki cv. "Heishi"). Food Chemistry, 330, 127253 Food Chemistry. https://doi.org/10.1016/j.foodchem.2020.127253

Raman, N. M., & Ramasamy, S. (2017). Genetic validation and spectroscopic detailing of DHN-melanin extracted from an environmental fungus. *Biochemistry and Biophysics Reports*, *12*, 98–107. https://doi.org/10.1016/J.BBREP.2017.08.008

Reiss, R. , Ihssen, J. , Richter, ., Eichhorn, E. , & Schilling, B. & T.-M. L. (2013). Laccase versus Laccase-Like Multi-Copper Oxidase: A Comparative Study of Similar Enzymes with Diverse Substrate Spectra. PLoS ONE, 8(6)

Restaino, O.F.; Manini, P.; Kordjazi, T.; Alfieri, M.L.; Rippa, M.; Mariniello, L.; Porta, R. (2024) Biotechnological production and characterization of extracellular melanin by *Streptomycesnashvillensis*. *Microorganisms*, *12*, 297.

Restaino, O.F.; Scognamiglio, M.; Mirpoor, S.F.; Cammarota, M.; Ventriglia, R.; Giosafatto, C.V.L.; Fiorentino, A.; Porta, R.; Schiraldi, C. (2022) Enhanced *Streptomyces roseochromogenes* melanin production by using the marinerenewablesource *Posidonia oceanica* egagropili. *Appl. Microbiol. Biotechnol.*, *106*, 7265–7283

Ribera J, Panzarasa G, Stobbe A et al (2019) Scalable biosynthesis of melanin by the basidiomycete Armillaria cepistipes. J Agric Food Chem 67:132–139. https://doi.org/10.1021/acs.jafc.8b05071

Rudrappa, M.; Kumar, M.S.; Kumar, R.S.; Almansour, A.I.; Perumal, K.; Nayaka, S. (2022), Bioproduction, purification, and physicochemical characterization of melanin from Streptomyces sp. strain MR28. Microbiol. Res. 263, 127130

Saber, W.I.A., Ghoniem, A.A., Al-Otibi, F.O. *et al.* (2023). A comparative study using response surface methodology and artificial neural network towards optimized production of melanin by *Aureobasidium pullulans* AKW. *Sci Rep* 13, 13545 https://doi.org/10.1038/s41598-023-40549-z

Saini, A. S. , & & Melo, J. S. (2015). One-pot green synthesis of eumelanin: process optimization and its characterization. RSC Advances, 5(59), 47671–47680 RSC Advances. https://doi.org/10.1039/c5ra01962a

Sajjan, S., Kulkarni, G., Yaligara, V., Kyoung, L., and Karegoudar, T. B. (2010). Purification and Physiochemical Characterization of Melanin Pigment from Klebsiella Sp. GSK. *J. Microbiol. Biotechnol.* 20, 1513–1520. doi:10.4014/jmb.1002.02006

Schmaler-Ripcke, J. , Sugareva, V. , Gebhardt, P. , Winkler, R. , Kniemeyer, O. , Heinekamp, T. , & Brakhage, A. A. (2008). Production of Pyomelanin, a Second Type of Melanin, via the Tyrosine Degradation Pathway in *Aspergillus fumigatus*. Applied and Environmental Microbiology, 75(2), 493–503 Applied and Environmental Microbiology. https://doi.org/10.1128/AEM.02077-08

Sendovski, M. , Kanteev, M. , Ben-Yosef, V. S. , & Adir, N. & F. A. (2011). First Structures of an Active Bacterial Tyrosinase Reveal Copper Plasticity. Journal of Molecular Biology, 405(1), 227–237 https://doi.org/10.1016/j.jmb.2010.10.048

Shams Yazdani, S., & Gonzalez, R. (2008). Engineering Escherichia coli for the efficient conversion of glycerol to ethanol and co-products. *Metabolic Engineering*, *10*(6), 340–351. https://doi.org/10.1016/J.YMBEN.2008.08.005

Silveria, S. T. , Daroit, D. J. , & Brandelli A. (2008, January 18). Pigment production by *Monascus purpureus* in grape waste using factorial design. LWT - Food Science and Technology, 41(1), 170–174 Food Science and Technology. https://doi.org/10.1016/j.lwt.2007.01.013

Singh, S., Nimse, S. B., Mathew, D. E., Dhimmar, A., Sahastrabudhe, H., Gajjar, A., Ghadge, V. A., Kumar, P., & Shinde, P. B. (2021). Microbial melanin: Recent advances in biosynthesis, extraction, characterization, and applications. *Biotechnology Advances*, *53*, 107773. https://doi.org/10.1016/J.BIOTECHADV.2021.107773

Solano, F. (2014). Melanins: Skin Pigments and Much More—Types, Structural Models, Biological Functions, and Formation Routes. *New Journal of Science*, *2014*, 1–28. https://doi.org/10.1155/2014/498276

Solano, F. (2017). Melanin and Melanin-Related Polymers as Materials with Biomedical and Biotechnological Applications-Cuttlefish Ink and Mussel Foot Proteins as Inspired Biomolecules. *International Journal of Molecular Sciences*, *18*(7). https://doi.org/10.3390/IJMS18071561

Srisuk, P., Correlo, V. M., Leonor, I. B., Palladino, P., & Reis, R. L. (2015). Effect of Melanomal Proteins on Sepia Melanin Assembly. *Journal of Macromolecular*

Science, Part B, *54*(12), 1532–1540. https://doi.org/10.1080/00222348.2015.1103430

Strube, O. I., Büngeler, A., & Bremser, W. (2015). Site-specific in situ synthesis of eumelanin nanoparticles by an enzymatic autodeposition-like process. *Biomacromolecules*, *16*(5), 1608–1613. https://doi.org/10.1021/ACS.BIOMAC.5B00187/SUPPL_FILE/BM5B00187_SI_001.PDF

Sun, S. , Zhang, X. , Chen, W. , Zhang, L. , & & Zhu, H. (2016). Production of natural edible melanin by *Auricularia auricula* and its physicochemical properties. Food Chemistry, 196, 486–492 Food Chemistry. https://doi.org/10.1016/j.foodchem.2015.09.069

Surwase, S. N. , Jadhav, S. B. , Phugare, S. S., & & Jadhav, J. P. (2012). Optimization of melanin production by *Brevundimonas sp. SGJ* using response surface methodology. 3 Biotech, 3(3), 187–194 Biotech. https://doi.org/10.1007/s13205-012-0082-4

Surwase, S. N., Patil, S. A., Apine, O. A., & Jadhav, J. P. (2012). *Efficient Microbial Conversion of l-Tyrosine to l-DOPA by Brevundimonas sp. SGJ. Applied Biochemistry and Biotechnology, 167(5), 1015–1028.* doi:10.1007/s12010-012-9564-4

Swann, G. E. A., & Patwardhan, S. V. (2011). Application of Fourier Transform Infrared Spectroscopy (FTIR) for assessing biogenic silica sample purity in geochemical analyses and palaeoenvironmental research. *Climate of the Past*, *7*(1), 65–74. https://doi.org/10.5194/CP-7-65-2011

Tarangini K. , Susmita Mishra. (2014). Production of melanin by soil microbial isolate on fruit waste extract: two step optimization of key parameters, department of Chemical Engineering, National Institute of Technology, Rourkela 769 008, Orissa, India

Toledo, A. V. , Franco, M. E. E. , Yanil Lopez, S. M. , Troncozo, M. I. , Saparrat, M. C. N. , & Balatti, P. A. (2017). Melanins in fungi: Types, localization and putative biological roles. Physiological and Molecular Plant Pathology, 99, 2–6 Physiological and Molecular Plant Pathology. https://doi.org/10.1016/j.pmpp.2017.04.004

Tran-Ly, A. N., Reyes, C., Schwarze, F. W. M. R., & Ribera, J. (2020). Microbial production of melanin and its various applications. *World Journal of Microbiology and Biotechnology*, *36*(11), 1–9. https://doi.org/10.1007/S11274-020-02941-Z/FIGURES/3

Turick, C. E., Tisa, L. S., & Caccavo, F. (2002). Melanin production and use as a soluble electron shuttle for Fe(III) oxide reduction and as a terminal electron acceptor by Shewanella algae BrY. *Applied and Environmental Microbiology*, *68*(5), 2436–2444. https://doi.org/10.1128/AEM.68.5.2436-2444.2002

Udaka, S. (1960). Screening method for microorganisms accumulating metabolites and its use in the isolation of Micrococcus glutamicus. *Journal of Bacteriology*, *79*(5), 754–755. https://doi.org/10.1128/JB.79.5.754-755.1960

Valıpour E., Arıkan B. (2015). Optimization of Tyrosinase Enzyme Production from Native Bacillus sp. MV29 Isolate. Journal of Applied Biological Sciences, 77-82

Wakamatsu, K., Fujikawa, K., Zucca, F. A., Zecca, L., & Ito, S. (2003). The structure of neuromelanin as studied by chemical degradative methods. *Journal of Neurochemistry*, *86*(4), 1015–1023. https://doi.org/10.1046/J.1471-4159.2003.01917.X

Wang L, Li Y, Li Y (2019) Metal ions driven production, characterization and bioactivity of extracellular melanin from Streptomyces sp. ZL-24. Int J Biol Macromol 123:521–530. https://doi. org/10.1016/j.ijbiomac.2018.11.061

Yang, J. , Li, W. , Ng, T. B. , Deng, X. , & Lin, J. & Y. X. (2017). Laccases: Production, Expression Regulation, and Applications in Pharmaceutical Biodegradation. Frontiers in Microbiology, 8 https://doi.org/10.3389/fmicb.2017.00832

Yousuf, A., Pirozzi, D., & Sannino, F. (2019). Fundamentals of lignocellulosic biomass. *Lignocellulosic Biomass to Liquid Biofuels*, 1–15. https://doi.org/10.1016/B978-0-12-815936-1.00001-0

Zhou, C. H., Xia, X., Lin, C. X., Tong, D. S., & Beltramini, J. (2011). Catalytic conversion of lignocellulosic biomass to fine chemicals and fuels. *Chemical Society Reviews*, *40*(11), 5588–5617. https://doi.org/10.1039/C1CS15124J

Zou, Y. , & Tian, M. (2016). Fermentative Production of Melanin by *Auricularia auricula* . Journal of Food Processing and Preservation, 41(3), e12909 Journal Food Processing and Preservation. https://doi.org/10.1111/jfpp.12909

Zou, Y., & Hou, X. (2017). Optimization of culture medium for production of melanin by Auricularia auricula. Food Science and Technology, 37(1), 153–157. doi:10.1590/1678-457x.18016

APPENDIX A – Raw data on Cg-EKV-I

For each raw data, different copper ions, different volume of production, and purification of melanin with different conditions were tabled.

Table A.1: Raw data for different copper ions on Cg-EKV-I

Time of copper addition (hour)	Cu (mM)	Titer (g/L)
24	0.1	0.59
		0.43
	0.2	0.72
		0.46
	0.25	0.84
		0.75
	0.3	0.85
		0.75
	0.4	0.92
		0.42
	0.6	0.44
		0.54
48	0.1	0.64
		0.84
		0.77
	0.2	0.68
		0.92
		0.82
	0.25	0.91
		0.81
		0.80
	0.3	0.93
		0.83
		0.90

	0.4	0.70
		0.89
		0.67
	0.6	0.64
		0.54
		0.40
72	0.1	0.73
		0.92
		0.77
	0.2	0.76
		0.96
		0.81
	0.25	0.93
		0.83
		0.90
	0.3	0.95
		0.90
		0.85
	0.4	0.80
		0.91
		0.62
	0.6	0.44
		0.64
		0.70

Table A.2: Raw data for different volume of production effect on Cg-EKV-I

Time (hour)	Volume of production (mL)	Titer (g/L)
24	25	0.72
		2.44
		0.53
		0.37
	50	1.17
		1.17
		0.50
		0.43
	75	0.54
		0.54
		0.26
		0.26
48	25	0.95
		0.95
		0.95
		0.90
	50	0.84
		0.88
		0.87
		0.84
	75	0.50
		0.50
		0.81
		0.77
72	25	0.98
		0.94
		1.01
		0.94

72	50	0.88
		0.91
		0.94
		0.89
	75	0.85
		0.89
		0.81
		0.81

Table A.3: Raw data the yields result from the purification of melanin for Cg-EKV-I with different growth conditions.

Volume (mL)	**Rpm**	**Yield (mg Mel / mg Tyr)**
50	150	0.192
		0.179
		0.229
25		0.226
		0.047
		0.855
50	180	0.176
		0.205
25		0.05
		0.302

APPENDIX B – Kriging and Quadratic model selected data

The selected data for Kriging and Quadratic models were given in tables.

Table B.1: Kriging model selected data

Time of copper addition (hour)	**Cu (mM)**	**L-Phe (mM)**
5	0.12	0.18
5	0.12	0.42
5	0.33	0.18
5	0.33	0.42
19	0.12	0.18
19	0.12	0.42
19	0.33	0.18
19	0.33	0.42
0	0.23	0.30
24	0.23	0.30
12	0.05	0.30
12	0.40	0.30
12	0.23	0.10
12	0.23	0.50
12	0.23	0.30
12	0.23	0.30
12	0.23	0.30
12	0.23	0.30
12	0.23	0.30
12	0.23	0.30
12	0.23	0.30
12	0.23	0.30
12	0.23	0.30
12	0.23	0.30
12	0.23	0.30

Table B.2: Quadratic model selected data

Time of copper addition (hour)	Cu (mM)	L-Phe (mM)
0.5	0.07	0.20
13.3	0.14	0.40
6.3	0.33	0.36
3.3	0.18	0.12
16.3	0.10	0.50
19.6	0.24	0.24
5.7	0.22	0.28
14.2	0.29	0.33
23.9	0.28	0.38
10.6	0.36	0.45
20.5	0.39	0.21
9.1	0.12	0.15

APPENDIX C – OD_{600} results

Below, the OD_{600} results of Kriging and Quadratic models were given in tables. It is announced in the table titles which OD_{600} results fits to which tables in the results section.

Table C.1: Kriging model OD_{600} results from Table 3.12.

Time of copper addition (hour)	Cu (mM)	L-Phe (mM)	24	48	72
0	0.23	0.30	5.87	14.6	18.7
5	0.12	0.42	25.5	25.1	32.7
5	0.33	0.18	15.6	24.2	21
5	0.33	0.42	10.06	24	28
5	0.23	0.30	10.24	16.7	15.8
12	0.05	0.30	16.8	21	30.3
12	0.40	0.30	15.3	21.3	36.6
12	0.23	0.30	18.6	23.2	45.8
12	0.23	0.30	18.16	25.7	23.1
12	0.23	0.30	30.5	34.5	32.9
12	0.23	0.30	12.12	23.2	22.5
12	0.23	0.30	15.74	21.5	20.3
12	0.23	0.30	16.14	22.1	18.1
12	0.23	0.30	17.3	13.3	21.7
12	0.23	0.30	16	18.9	39.1
12	0.40	0.30	12.32	25	22.2
12	0.23	0.30	15.1	25.7	22.6
12	0.12	0.18	15.84	13.2	21.7
12	0.23	0.30	16.3	24	36.3
19	0.12	0.18	9.24	16.5	21.7
19	0.12	0.42	25.3	34	34.7
19	0.33	0.18	10.9	18.3	18.7
19	0.33	0.42	25.8	36.1	40.7
24	0.23	0.30	13.38	25.5	22

Table C.2: Quadratic model OD_{600} results from Table 3.13.

Time of copper addition (hour)	Cu (mM)	L -Phe (mM)	24	48	72
0.5	0.07	0.20	7.03	13.26	10.5
0.5	0.07	0.20	9.32	11.66	12.7
0.5	0.07	0.20	7.34	19.9	19.5
3.3	0.18	0.12	7.52	8.78	8.32
3.3	0.18	0.12	7.38	7.5	7.43
3.3	0.18	0.12	7.64	7.5	8.23
5.7	0.22	0.22	14.9	18.3	22
5.7	0.22	0.28	12.8	21.84	25
5.7	0.22	0.28	13.2	19.32	22.6
6.3	0.33	0.36	25.4	26.3	31.2
6.3	0.33	0.36	22.5	25.6	32.1
6.3	0.33	0.36	19.6	26.9	23.4
10.6	0.36	0.45	28.4	35.9	32.5
10.6	0.36	0.45	31.9	31.2	31.9
10.6	0.36	0.45	31.8	34.5	30.8
13.3	0.14	0.40	23.6	25.4	24
13.3	0.14	0.40	23.7	26.1	25.7
13.3	0.14	0.40	23.8	24	26
14.2	0.29	0.33	15.1	18	20.8
14.2	0.29	0.33	16.9	17.6	21.7
14.2	0.29	0.33	14	16.9	22.5
16.3	0.1	0.5	29.7	28.3	22.7
16.3	0.1	0.5	28.5	27.7	21.9
16.3	0.1	0.5	27.5	26.6	21.8
19.6	0.24	0.24	9.36	21.7	18.7
19.6	0.24	0.24	8.7	20.8	17.7
19.6	0.24	0.24	9.5	21.5	16.9
20.5	0.39	0.21	7.57	9.55	12.3
20.5	0.39	0.21	6.9	9.8	11.9
20.5	0.39	0.21	8.1	10.1	13.1
23.9	0.28	0.38	25.7	31.2	32.5
23.9	0.28	0.38	35.8	33.3	21.9
23.9	0.28	0.38	35.5	33.9	36.4

APPENDIX D – HPLC results

All the Hplc results from result section in 3.5.1.

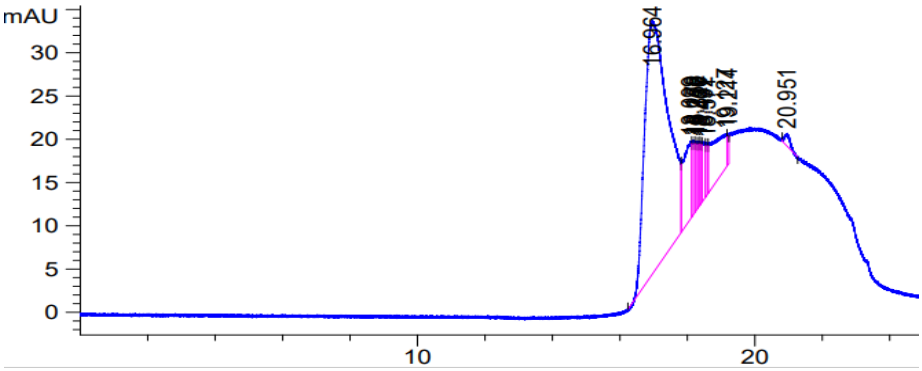

Figure D.1: Melanin analysis with HPLC at 25 °C

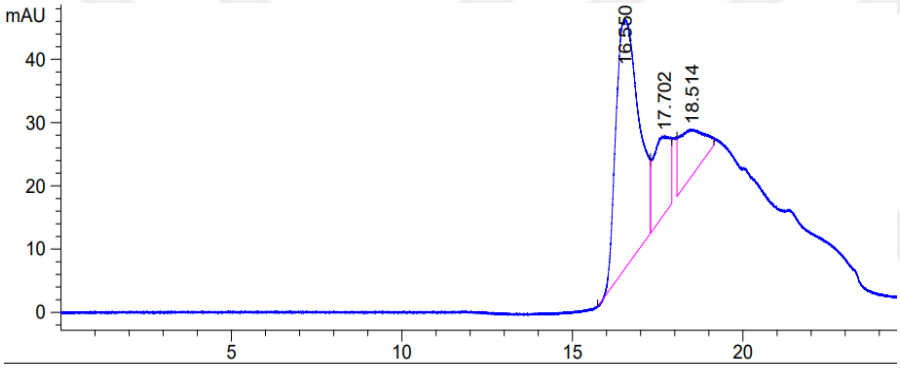

Figure D.2: Melanin analysis with HPLC at 35 °C

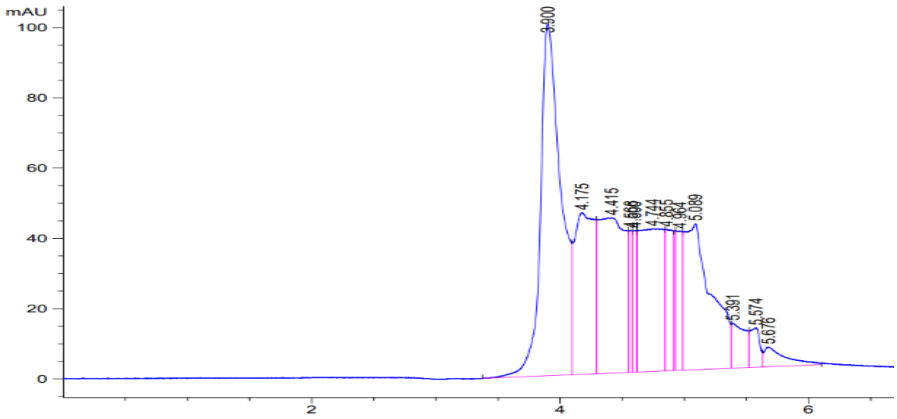

Figure D.3: Melanin analysis with HPLC at 70 °C

CURRICULUM VITAE /ÖZGEÇMİŞ

Ceren KARCIOĞLU

EDUCATION

2021– 2024 **Master's Degree**: Marmara University, Faculty of Engineering, Istanbul Department of Bioengineering.

Thesis*:* Tyrosinase-based melanin production in *Corynebacterium glutamicum*

2016 – 2021 **Bachelor**: Marmara University, Faculty of Engineering, Istanbul Department of Bioengineering.

2012 – 2016 **Highschool**: Era College, Adana

EXPERIENCE

July 2019 Istanbul University Capa Medicine Faculty

BOS laboratory**,** İstanbul, *Summer Internship*

June 2020 Cadde Veterinary**,** Laboratory, İstanbul, *Summer Internship*

ADDITIONAL INFORMATION

Project participation: TUBITAK grant on: Rasyonel Tasarım ile *Corynebacterium glutamicum'un* L-Dopa Üretimi için Bir Mikrobiyal Hücre Fabrikasına Dönüştürülmesi ve L-Dopa Üretim Prosesinin Geliştirilmesi

Conference: 6th International Eurasian Conference on Biological and Chemical Sciences (EurasianBioChem 2023)

Languages: English: B2

Computer: SuperPro Designer, proficient user in MS Office

Interests: Cosmetic production, beauty